

University of Windsor

Scholarship at UWindor

Electronic Theses and Dissertations

Theses, Dissertations, and Major Papers

1-1-1986

Glaciotectonic folding of a chalk-diamicton sequence from Hvideklint, Mon, Denmark.

David Alexander Coyle
University of Windsor

Follow this and additional works at: <https://scholar.uwindsor.ca/etd>

Recommended Citation

Coyle, David Alexander, "Glaciotectonic folding of a chalk-diamicton sequence from Hvideklint, Mon, Denmark." (1986). *Electronic Theses and Dissertations*. 6794.
<https://scholar.uwindsor.ca/etd/6794>

This online database contains the full-text of PhD dissertations and Masters' theses of University of Windsor students from 1954 forward. These documents are made available for personal study and research purposes only, in accordance with the Canadian Copyright Act and the Creative Commons license—CC BY-NC-ND (Attribution, Non-Commercial, No Derivative Works). Under this license, works must always be attributed to the copyright holder (original author), cannot be used for any commercial purposes, and may not be altered. Any other use would require the permission of the copyright holder. Students may inquire about withdrawing their dissertation and/or thesis from this database. For additional inquiries, please contact the repository administrator via email (scholarship@uwindsor.ca) or by telephone at 519-253-3000ext. 3208.

NOTE TO USERS

This reproduction is the best copy available.

UMI[®]

GLACIOTECTONIC FOLDING OF A
CHALK-DIAMICTON SEQUENCE FROM
HVIDEKLINT, MØN, DENMARK

by

David Alexander Coyle

A Thesis
submitted to the Faculty of Graduate Studies
through the Department of
Geology in Partial Fulfillment
of the Degree of
Master of Science at
The University of Windsor

Windsor, Ontario, Canada

1986

UMI Number: EC54781

INFORMATION TO USERS

The quality of this reproduction is dependent upon the quality of the copy submitted. Broken or indistinct print, colored or poor quality illustrations and photographs, print bleed-through, substandard margins, and improper alignment can adversely affect reproduction.

In the unlikely event that the author did not send a complete manuscript and there are missing pages, these will be noted. Also, if unauthorized copyright material had to be removed, a note will indicate the deletion.

UMI[®]

UMI Microform EC54781
Copyright 2010 by ProQuest LLC
All rights reserved. This microform edition is protected against
unauthorized copying under Title 17, United States Code.

ProQuest LLC
789 East Eisenhower Parkway
P.O. Box 1346
Ann Arbor, MI 48106-1346

LIST OF TABLES

Table 2.1	Pleistocene Stratigraphy at Scarborough...	19
Table 3.1	AMS Data from Hvideklint.....	43
Table 3.2	AMS Fabric Data from Hvideklint.....	46
Table 3.3	Pebble Fabric Data from Hvideklint.....	50
Table 3.4	Block Mean Remanence Data from Hvideklint.	57
Table 3.5	AMS Data from Scarborough.....	65
Table 3.6	AMS Fabric Data from Scarborough.....	66

LIST OF PLATES

Plate 3.1	Contact Between the Glaciotectonic Microbreccia and Underlying Undeformed Sands, Hvideklint.....	34
Plate 3.2	Undeformed Sands Below the Glaciotectonic Microbreccia, Hvideklint.....	35
Plate 3.3	Preserved Sedimentary Lamination in Block HK84-13, Hvideklint.....	40
Plate 3.4	Pseudo-drag folds at Hvideklint.....	41
Plate 3.5	Centre of the Scarborough Flow Fold.....	69
Plate 4.1	Random Orientation of Flint Nodules in the Central Deformed Chalk at Hvideklint..	85
Plate 4.2	Detail of the Chalk-diamicton Contact.....	86
Plate 4.3	Deformations in an Outwash-diamicton Sequence Southwest of Hvideklint.....	90
Plate 4.4	Deformations above those Pictured in Plate 4.3.....	91
Plate 4.5	Folding in a Diamicton Sequence Northwest of Møns Klint.....	92
Plate 4.6	Folding in a Diamicton Sequence Northwest of Møns Klint.....	93
Plate 4.7	Diamicton Dike, Hvideklint.....	94
Plate 4.8	Gradational Contact between Chalk and Diamicton, Hvideklint.....	95

LIST OF FIGURES

Figure 2.1	Map of Denmark.....	8
Figure 2.2	Location of the Hvideklint Section.....	9
Figure 2.3	Location of the Scarborough Section.....	10
Figure 2.4	Sample Locations, Hvideklint.....	23
Figure 2.5	Sample Locations, Scarborough.....	24
Figure 2.6	Subsampling Procedure for the Hvideklint Specimens.....	25
Figure 3.1	Field Sketch, Hvideklint Section.....	32
Figure 3.2	Sketch of the area immediately adjacent to the unit sampled at Hvideklint.....	33
Figure 3.3	Sketch of the Folded Unit, Hvideklint....	38
Figure 3.4	Fold Axes and Poles to Bedding, Hvideklint.....	39
Figure 3.5	Stereoplot of Kmax Directions, Hvideklint.....	47
Figure 3.6	Stereoplots of Kmax Directions, Block HK84-09.....	48
Figure 3.7	Pebble orientations, Hvideklint.....	51
Figure 3.8	Step Demagnetisation Data, Hvideklint....	54
Figure 3.9	Remanence Directions, Hvideklint.....	55
Figure 3.10	Block Mean Remanence Directions, Hvideklint.....	56
Figure 3.11	Grain Size Distributions.....	60
Figure 3.12	Pebble Lithologies, Hvideklint.....	61
Figure 3.13	Carbonate Content, Hvideklint.....	62
Figure 3.14	Stereoplots of Kmax Directions, Scarborough.....	67
Figure 3.15	Distribution of A.M.S. Ellipsoid Shapes in Block SB85-05.....	68
Figure 4.1	Synoptic Fabric Diagram, Hvideklint.....	79
Figure 4.2	Distribution of Ellipticities in both the Hvideklint and Scarborough Folds.....	80
Figure 4.3	The Relationship between Subglacial Stresses and Glaciotectonic Folding (From Rotnicki, 1976).....	87
Figure 4.4	Model of the Origin of the Folding at Hvideklint.....	103

TABLE OF CONTENTS

ABSTRACT.....	vi
ACKNOWLEDGEMENTS.....	v
LIST OF FIGURES.....	iii
LIST OF PLATES.....	ii
LIST OF TABLES.....	i
1 Foreword.....	1
2 Introduction.....	2
2.1 Purpose.....	2
2.2 Terminology.....	4
2.3 Field Locations.....	7
2.4 Previous Work.....	11
Local Geology: Møn.....	14
Geology of the Scarborough Section.....	17
2.5 Sampling Procedures.....	20
2.6 Laboratory Methods.....	26
3 Field Observations and Laboratory Results.....	30
Hvideklint Section	
3.1 Stratigraphy.....	30
3.2 Structure.....	36
3.3 Anisotropy of Magnetic Susceptibility...	42
3.4 Pebble Fabrics.....	49
3.5 Paleomagnetism.....	52
3.6 Mechanical Analysis.....	58
Scarborough Section	
3.7 Anisotropy of Magnetic Susceptibility...	63
3.8 Mechanical Analysis.....	70
4 Interpretation of the Hvideklint Section.....	71
4.1 Origin of the Stratified Sequence.....	71
4.2 State of Strain.....	75
4.3 Mechanism of Folding at Hvideklint.....	81
4.4 Associated Deformations.....	88
4.5 Frozen or Unfrozen?.....	96
4.6 Model of the Origin of the Sequence at Hvideklint.....	100
5 Conclusions.....	104
REFERENCES.....	106
APPENDIX I	
Selected Bibliography.....	111
VITA AUCTORIS.....	116

ACKNOWLEDGEMENTS

The author thanks Dr. C.P. Gravenor for his assistance, both financial and critical, in the preparation of this thesis. Dr. D.T.A. Symons assisted with critical reading of the manuscript.

I also thank Andrew Bourque who performed one of the pebble analyses and one of the grain size analyses and Russel Reid who performed the carbonate content measurements and the pebble lithology count, and Elaine Coyle who assisted with some of the measurements of the A.M.S.

I also thank the Government of Ontario which provided me with a generous scholarship and the University of Windsor which provided further financial assistance.

The glaciotectonic deformation model of Rotnicki (1976) was employed. This model requires that deformation occurs beneath the ice proximal to the margin of the glacier. The ductile nature of the folds, the deformation properties of chalk-like materials and the location near the margin of the advancing ice suggest that the sequence was not frozen at the time of folding. Other folds from the vicinity of the Hvideklint and from the northeast coast of Møn demonstrate that the type of folding described at Hvideklint is not unique.

GLACIOTECTONIC FOLDING OF A CHALK-DIAMICTON
SEQUENCE FROM HVIDEKLINT, MØN, DENMARK

ABSTRACT

by

David Alexander Coyle

A Late Weichselian glaciotectonically folded sequence of Pleistocene diamicton, overlying outwash sands and silts, and displaced Cretaceous chalk was examined at the southwest end of the Hvideklint on the island of Møn in southeast Denmark. A detailed investigation of the deformation history of the sequence employed 229 measurements of the anisotropy of magnetic susceptibility, six pebble-orientation fabrics from a total of 262 pebbles, paleomagnetic remanence directions from 42 specimens and four mechanical analyses. The results were compared with the variation in the anisotropy of magnetic susceptibility of 200 specimens collected from within a single flow fold in a debris flow from the Sunnybrook Drift (Wisconsinan) at Scarborough, Ontario, Canada.

Using the anisotropy of magnetic susceptibility as an indicator of relative strain variation within the two folded sequences, it is shown that the Hvideklint sequence exhibits a pattern of strain distribution similar to that observed in the Scarborough flow fold. It is concluded that the folding in the chalk-diamicton sequence was the result of ductile flow of the chalk in response to dominantly lateral stresses created by the readvance of the Late Weichselian ice.

c David Alexander Coyle 1986
all rights reserved

ix

858076

1 FOREWORD

The study of glaciotectionic phenomena has been going on for almost a century. While many significant results have been obtained, the mechanisms by which glaciers can remove and transport huge blocks of preexisting rock remain somewhat elusive. So spectacular are some of the exposures of glaciotectionic thrusting that other glaciotectionic phenomena, particularly folding, may receive less attention than they merit. The following thesis shows how misinterpretations may arise when these glaciotectionic folds are not given detailed scrutiny.

2 INTRODUCTION

2.1 Purpose

The glaciotectonically disturbed Pleistocene drift sequences of southeastern Denmark are among the best described in the world. Although much attention has been paid to the origin of the larger-scale features, little work has been done on the smaller-scale details of the structures. In particular, only a few fabric analyses of specific glaciotectonic features have been made. It was therefore considered appropriate to carry out a detailed examination of a folded chalk-diamict sequence at the western end of Hvideklint, Møn, Denmark.

The methodology concentrated on the structural, physical and textural aspects of a deformed diamicton within this sequence. Because data from other sources concerning the behaviour of folded diamictons are sparse, a fold in a debris-flow from the Scarborough Bluffs, Ontario, was also examined. The results of this investigation should aid in the interpretation of the deformational environment of the Hvideklint diamicton.

This study shows that detailed analyses are required for an accurate interpretation of the environment and history of folded diamictons. The results also demonstrate that several sedimentological discrepancies exist in previous interpretations of the geology, and an attempt is

made to resolve these problems in light of the new data presented.

2.2 Terminology

The following is a list of terms and definitions used in this report, with brief notes on their usage.

Anisotropy of Magnetic Susceptibility: The AMS is a measure of the three-dimensional variation in the magnitude of the magnetic susceptibility of a rock or rock sample. It is a symmetric second-order tensor, and is in widespread use as an estimator of the microfabric of a rock (Rees, 1968; Hrouda, 1982).

Magnetic Fabric: The magnetic fabric is the rock fabric as determined by AMS. It is a more precise term than microfabric because a true microfabric would measure the orientations of all elongate elements within a certain size range, whereas magnetic fabric measures only magnetic materials. The magnetic fabric is not restricted to only elongate grains, but represents the net fabric whereby grains of all shapes and their net three principal axes are all measured.

Magnetic Foliation: The magnetic foliation is a mathematical expression which estimates the degree to which the AMS susceptibility ellipsoid approaches an oblate form. It is defined as:

$$100 * \frac{(((K1+K2) * 0.5) - K3)}{(K1+K2+K3)/3}$$

where K1, K2 and K3 are the magnitudes of the maximum, intermediate and minimum major semi-axes of the AMS ellipsoid (Tiara and Scholle, 1979).

Magnetic Lineation: The magnetic lineation is a measure of the degree to which the susceptibility ellipsoid approximates a prolate shape (Khan, 1962; Tiara and Scholle, 1979). It is defined as:

$$100 * \frac{(K1-K2)}{(K1+K2+K3)/3}$$

The magnetic foliation and lineation are referred to as the magnetic fabric parameters. There is a third fabric parameter, Q, which is the ratio of the magnetic lineation to the magnetic foliation (Hamilton and Rees, 1970).

Ellipticity: The ellipticity, E, is a measure of the overall shape of the AMS ellipsoid. It is defined as:

$$K2 * \frac{K2}{(K1*K3)}$$

When E is greater than 1.0, the ellipsoid is prolate in shape. When E is less than 1.0, the ellipsoid is oblate (Hrouda et al., 1971)

Kinetostratigraphy: A kinetostratigraphic drift unit is defined as: "the sedimentary unit deposited by an ice sheet or stream possessing a characteristic pattern and direction of movement" (Berthelsen, 1973). Care must be exercised when employing this principle in the field, however, because the individual drift units are not defined by lithology but by the orientation of the glacial forces which caused their emplacement.

2.3 Field Locations

The primary field work for this study was conducted on the island of Møn in south-eastern Sjælland, Denmark (Fig. 2.1). The samples were collected at the western end of the Hvideklint, approximately 1060 m west of the access lane at Ørebaksvej (Fig. 2.2). The map coordinates of this site are approximately 54°30'N latitude and 012°E longitude. The diamicton which was sampled is located approximately half way up a 20 m high cliff face.

Secondary field work was done on a section of the Scarborough Bluffs along Lake Ontario near Toronto, Canada. The sampled horizon is situated in a small ravine near the end of Sylvan Avenue (Fig. 2.3). The samples were collected from a diamicton at an elevation of approximately 47 m above lake level. The map coordinates of this site are 43° 43'N latitude and 79° 13'W longitude.

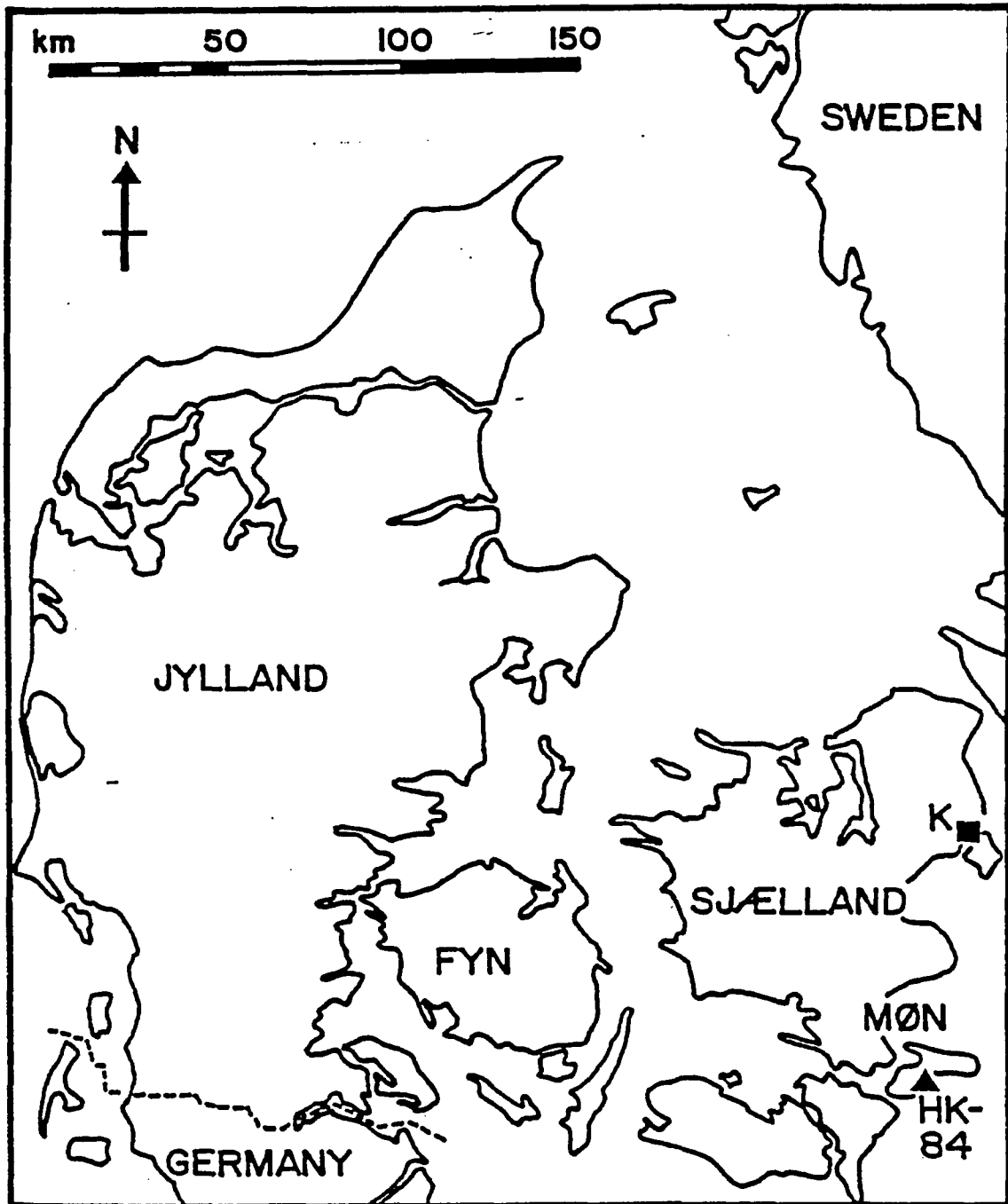


Figure 2.1 Map of Denmark.
Orientation map showing the location of the island of Møn,
Denmark. K is Copenhagen and HK84 is the sample locality.

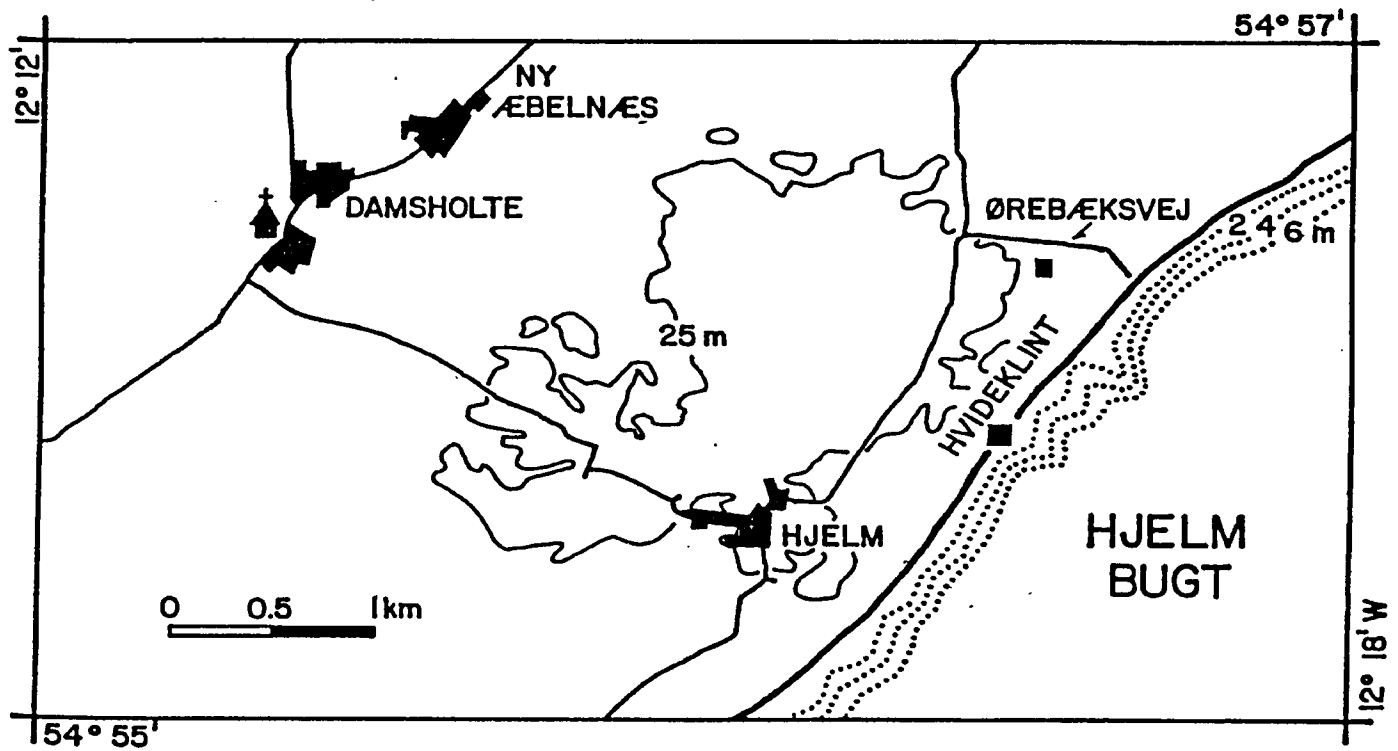


Figure 2.2 Location of the Hvideklint Section.

The solid square is sample locality HK84.

The contours indicate that the deformed complex extends both inland and seawards.

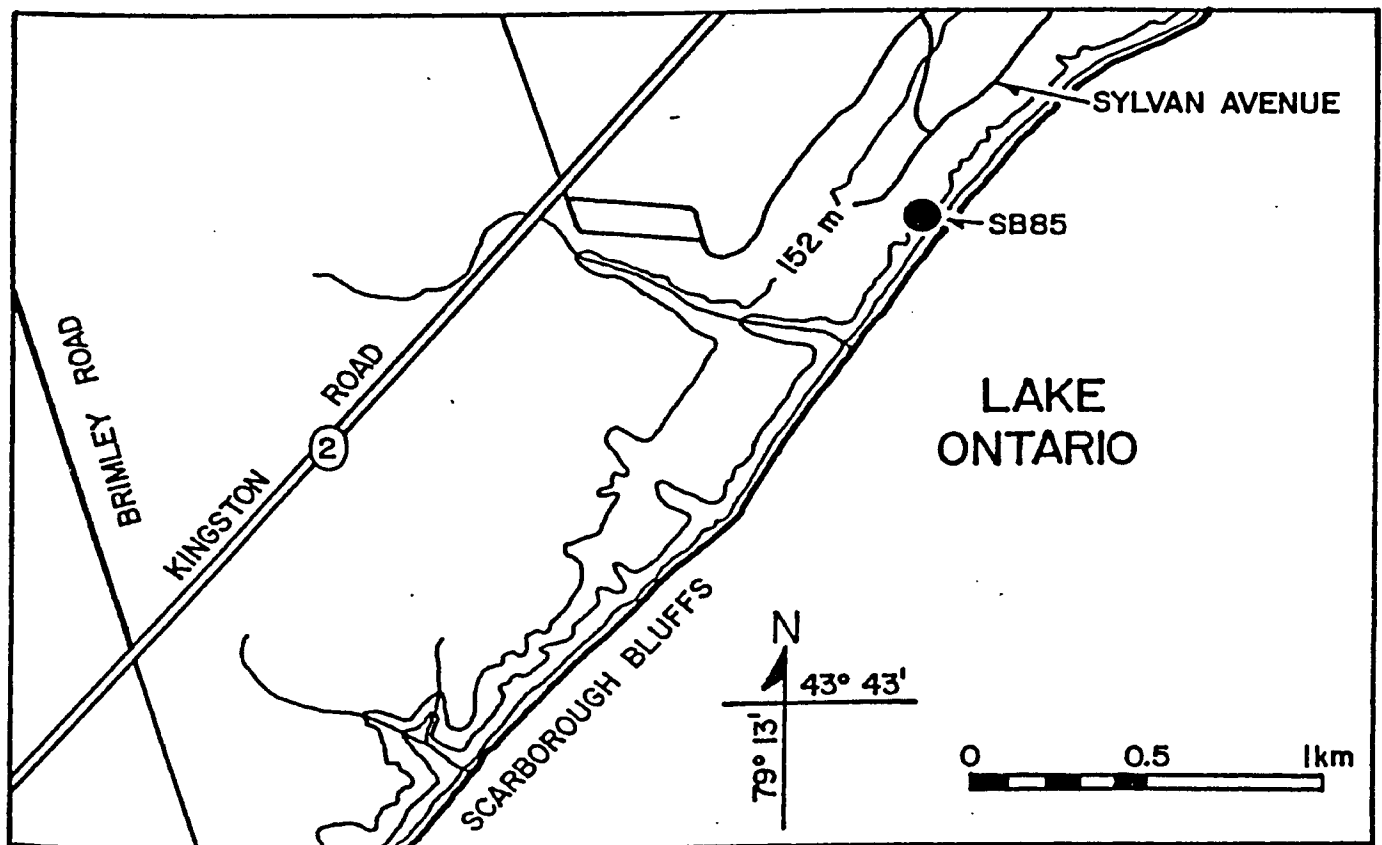


Figure 2.3 Location of the Scarborough Section.
The solid circle marks the sample locality SB85.

2.4 Previous Work

The Pleistocene of Denmark.

The major Quaternary glaciations of Denmark are correlatable with the Quaternary glaciations of North America (Woldstedt, 1954; Hansen, 1965). At the time of Hansen's (1965) review, the Danish Quaternary stratigraphers used either their own nomenclature or that of Alpine Central Europe. Since then the nomenclature of Northern Germany appears to have replaced the original Danish terminology. Thus, the Antepenultimate or Mindel Glaciation is now usually referred to as the Elster Glaciation which is the North German equivalent of the Kansan in North America. The most recent glaciation, the Weichselian (formerly the "Last Glaciation"), is equivalent to the Wisconsinan of North America according to Hansen (1965) and Woldstedt (1954). There is one problem with this correlation: the Wisconsinan of North America began much earlier than the Weichselian in Denmark although the two stadials ended at approximately the same time. Given this, it is probably fair to say that the Weichselian of Denmark is equivalent to only the Late Wisconsinan of North America.

The Weichselian began approximately 25 000 yBP (Berthelsen, 1979a) after the regression of the Skærumhede Sea, and is subdivided into three separate advances: the earliest Old Baltic Advance (the Norwegian Advance in

northern Denmark), the main North-East Ice Advance, and the Young Baltic Advance (replaced by the Younger Yoldia Sea in the north). Denmark was completely free of ice between each of these three advances. The Weichselian effectively ended in Denmark with the retreat of the Young Baltic ice and with the Bølling and Allerød climatic oscillations approximately 11-13 000 yBP (Berthelsen, 1979a). On the island of Møn, all three Late Weichselian stadials are represented and there is evidence for several readvances of the main North-East Ice Advance (Aber, 1980; Berthelsen, 1979a; Berthelsen et al., 1977; Sjørring, 1977).

Most of the more recent Quaternary stratigraphic work in Denmark centres on the use of the concept of kinetostratigraphy to classify and interpret the glaciotectionic sequences (Aber, 1980; Berthelsen, 1973, 1978, 1979a; Houmark-Nielsen & Berthelsen, 1981; Rasmussen, 1975). Application of this method in complete glacial sequences presents some problems because the assignment of proglacial and interstadial deposits to kinetic units in non-deformed sequences would be impossible or at least highly questionable. For this reason kinetostratigraphic classification is best used only in areas of complex deformation where all the sediments have been deformed by the ice in some manner.

The most effective application of the kinetostratigraphic approach is found in a study of the drift sequence of northern Samsø, Denmark, by

Houmark-Nielsen & Berthelsen (1981). They propose a standard chart for the presentation of kinetostratigraphic data which includes sections that detail the lithology of the section, the presence and orientations of any deformations, the till fabrics, and the paleocurrent directions for non-kinetic units. This sort of composite approach is superior because it recognises both the strengths and weaknesses of both the kinetic and lithostratigraphic methods. Where present, the kinetostratigraphic units are defined by characteristic fabrics and/or structures, and they are clearly differentiated from the non-kinetic units.

Local Geology: Møn.

The island of Møn is well known for its exposures of glaciotectonic features, the most famous of which are displayed in the prominent chalk cliffs of Møns Klint at the eastern end of the island. Another exposure, the Hvideklint on the central south coast of the island, has recently received some attention after a detailed examination by Aber (1980). "Typical" glaciotectonic features are found at this location, including: the emplacement of large allochthonous rafts of preglacial rock; the development of glaciotectonic mélange; and, the subsequent deformation of the emplaced sequence by overriding ice. One unique feature of this location is that the post-emplacement deformation is most pronounced on the lee side of the allochthon rather than on the stoss side with respect to the presumed direction of ice movement.

The local stratigraphy at Hvideklint consists of three till units with intervening chalk rafts and disturbed glacio-fluvial sediments. These tills are, from base to top, the Lower Dislocated Till, the Upper Dislocated Till and the upper Discordant Till (Aber, 1980). Aber (1980) suggested that the Lower Dislocated Till belongs to the Old Baltic advance, and that the Upper Dislocated Till and the Discordant Till belong to separate readvances of the main

North-East Advance. He stated that it is unlikely that the Discordant Till could belong to the Young Baltic Advance but offered little evidence to support this opinion.

The emplacement of the chalk must have occurred during the initial advance of the main North-East ice because the Upper Dislocated Till contains a large percentage of chalk and flint pebbles, containing up to 50% chalk. This is evidence for a syn- or post-chalk-emplacement time for the Upper Dislocated Till. Conversely, in the Lower Dislocated Till, the chalk and flint pebbles are notably lower at only 2.1% chalk (Aber, 1980). Thus if the assumption that the Lower Dislocated Till belongs to the Old Baltic Advance is valid, there is no evidence for a North-East advance prior to the emplacement of the chalk allochthon. This does not preclude the possibility of an early North-East Advance till having been deposited and then eroded away. The structural evidence associated with the chalk cliffs indicates that the allochthons were brought in from the northeast, which supports the hypothesis of Berthelsen (1979) that the ice brought the chalk over the island from the Fakse Bugt area. Previously, it had been thought that the ice advance was refracted about the eastern end of the island, causing the chalk at Hvideklint to be emplaced from the south (Hansen, 1965).

As no palynological work has been done on the unnamed glaciofluvial deposits found between the readvances of the North-East Ice, it is difficult to determine the nature of

the paleoclimate. Data taken from deposits which predate the North-East Advance indicate subarctic or tundra conditions (Hansen, 1965). There are no reported findings of wood or fossils in any of the Møn sections. Thus the general opinion of researchers working on these sections is that the sediments are undatable either by absolute dating methods such as C-14 or amino-acids, or by secondary dating methods such as paleomagnetism (A. Berthelsen, pers. comm.).

Geology of the Scarborough Section.

The Pleistocene geology of the Scarborough area consists almost entirely of deposits of the Wisconsinan glaciation. The local stratigraphy has been described and compiled by Karrow (1967), and is reproduced in Table 2.1. The sampled unit is a silty-clay which exhibits flow folding. It lies unconformably above the Sunnybrook Till Member and below the varved clays of the Bloor Member in the Sunnybrook Drift (Karrow, 1984b).

A recent re-interpretation of the depositional environment of the sediments found in the Scarborough Bluffs by Eyles and Eyles (1983) departs from the traditional concepts of till deposition. They assumed that the entire Sunnybrook sequence is the product of sedimentation in a large lake. Massive tills are interpreted to be the result of constant sediment rain-out from floating debris-laden ice with no current reworking. They interpreted the sampled unit to be a resedimented matrix-supported diamict that was formed as the result of subaqueous slumping on an irregular lake-bottom topography. This interpretation is questionable because it does not explain how the Sunnybrook Till could possess an irregular surface to induce the subaqueous slumping.

There is continuing controversy over the validity of the interpretations of Eyles and Eyles (1983) (e.g. Karrow, 1984a; Dreimanis, 1984). However, for the purposes of this study, the interpretation that the sampled unit is a

subaqueous flow deposit is not questioned because all authors agree on this point.

Table 2.1
Pleistocene Stratigraphy at Scarborough

FORMATIONS AND EVENTS

Stage	Formation or Event	lithology
Recent	Lake Ontario beaches	Beach, sand, gravel
	Alluvium	Clay, silt, sand, gravel
	Swamp and bog deposits Stream terrace deposits	Marl, muck, peat Clay, sand, gravel
Wisconsinan	Late	Lake Iroquois
		Early peripheral lakes
		<u>Leaside Till</u>
		Lake and stream deposits
		<u>Meadowcliffe Till</u>
		Lake and stream deposits
		<u>Seminary Till</u>
	Middle	<u>Thorncliffe Formation</u>
	Early	<u>Sunnybrook Drift</u> <u>Scarborough Formation</u>
Sangamonian	<u>Don Formation</u>	Clay, sand, wood
Illinoian	<u>York Till</u>	Clayey sand till

Formation names are underlined.
(Modified after Karrow, 1967.)

2.5 Sampling Procedures

Field sampling was carried out by excavating oriented blocks from the exposures. The blocks were collected as close as possible to one another. They represented a complete sequence through the folds with the hinges and limbs represented by separate blocks. The orientations of bedding and fold hinge axes were measured in the field. The Hvideklint section is of a sufficient size to allow a second set of blocks to be obtained, collected parallel to the first set, along the fold axes (Fig. 2.4). Unfortunately, the Sunnybrook site was not sufficiently extensive parallel to the fold axis to permit such duplicate sampling (Fig. 2.5). In both cases, the average size of each block was 15 cm in height, by 20 cm in width and by 20 cm in length.

Subsampling for AMS, pebble fabrics and paleomagnetic remanence was done in the laboratory. The specimens for AMS and paleomagnetic studies were obtained by carefully cutting out 2cm x 2cm x 2cm cubes of the sediment and placing them in snug-fitting styrene boxes with external dimensions of 2.54x2.54x2.54 cm. For the more clay-rich material from the Scarborough section, the containers were subsequently sealed to prevent loss of moisture which could result in the shrinkage of the specimens. The actual cutting of the specimens had to be undertaken with great

precision because forcing the container over a too-large specimen could produce deformation errors in the measurements for the specimen (Gravenor et al., 1984). Conversely, a too-small specimen would be free to rotate within the container which could introduce orientation errors. In all cases, the observed difference between the ideal and the actual dimensions of the specimens was less than 1 mm.

Two methods were employed to cut the specimens. The specimens from the Scarborough section were cut using a hobby knife similar to the procedure described in Gravenor et al. (1984). The Hvideklint sediment, however, contains a larger percentage of pebbles which made the collection of perfectly cubical specimens impossible. Furthermore, this sediment is also very clay-poor which precluded the use of the second common subsampling procedure which is the drilling of cores with a diamond-tipped bit. This type of drilling would have been impossible because the drill requires circulating water for lubricating, cooling, and removing the debris from the undrained drill hole. The clay content would not be high enough to prevent complete disaggregation of the sandy matrix of the sediment when it came into contact with the circulating water. A new method was devised (Fig. 2.6) where the large sample blocks were first dry cut into 5 cm thick slabs using a 25 cm diameter circular carborundum saw blade. The slabs were then sealed on their exposed faces using several coats of diluted

varnish. The varnish penetrated to a depth of at least 3 mm, and thus effectively waterproofed the slab. The rough slabs were then cut into 2 cm thick slabs using a 20 cm diameter water-lubricated circular diamond blade. The exposed faces were then sealed, and these small slabs cut and trimmed into 2x2x2 cm specimens again using the 20 cm diamond saw. The samples were then placed into the sample containers. Through all stages of this procedure orientation marks were kept on the slabs using waterproof ink.

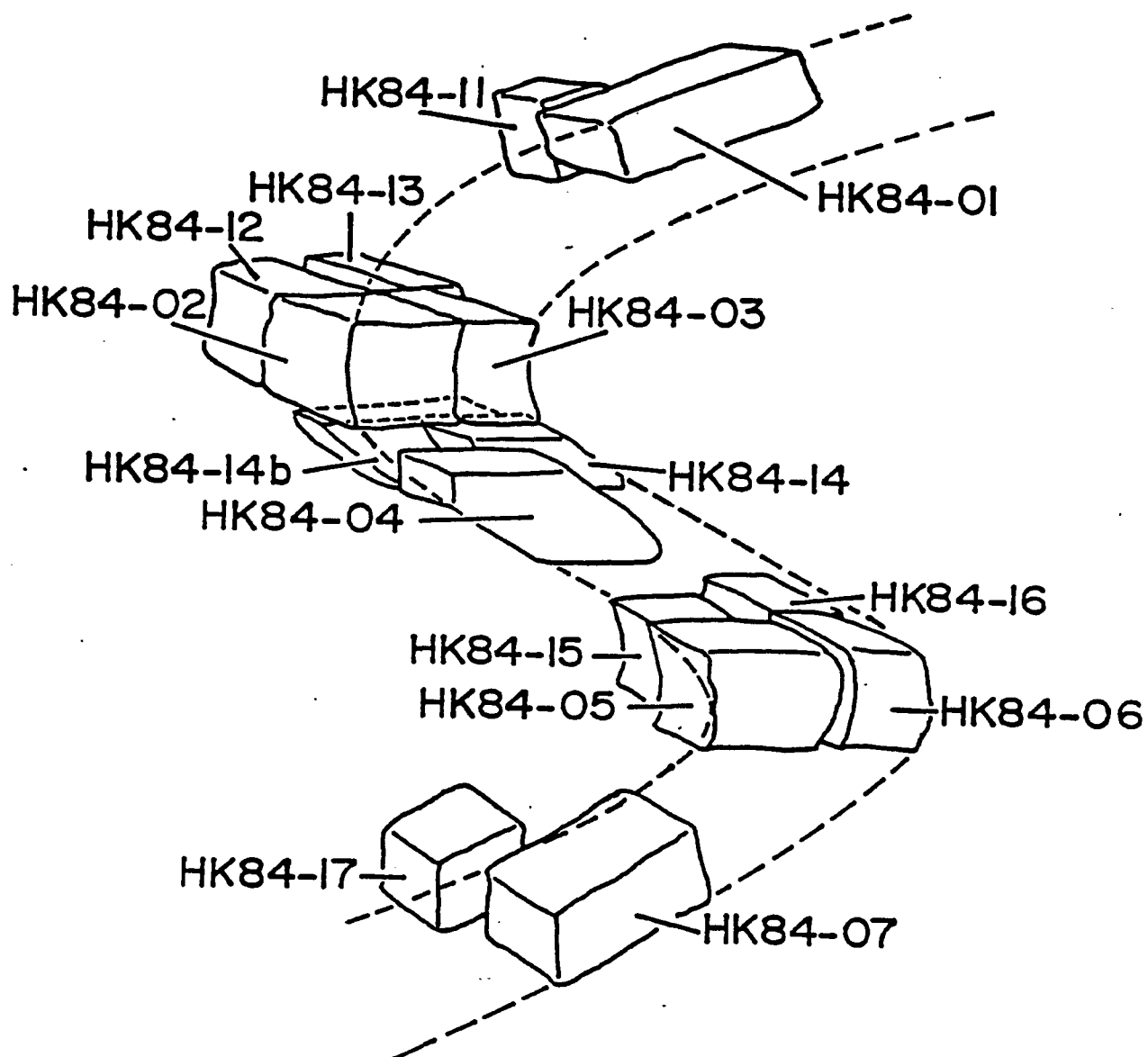


Figure 2.4 Sample Locations, Hvideklint
Schematic Section showing the locations of the samples obtained from the Hvideklint section. The dashed line outlines the trace of the fold.

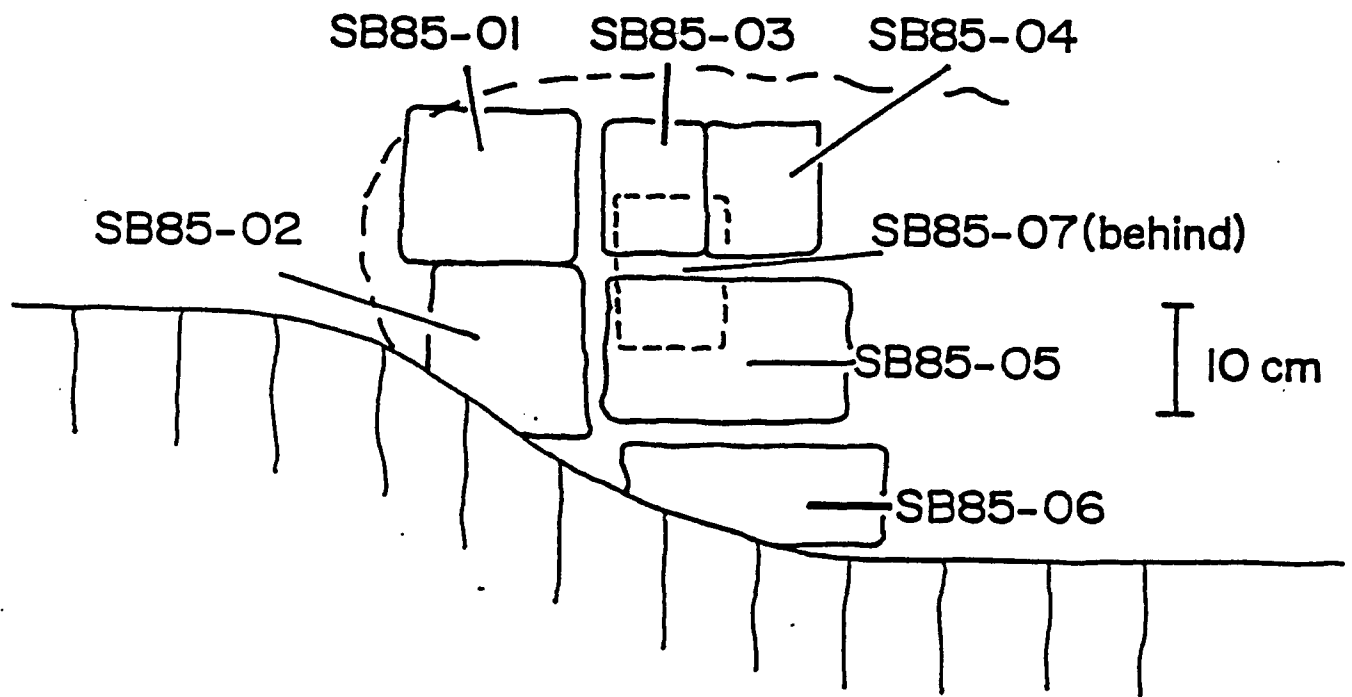


Figure 2.5 Sample Locations, Scarborough
 Schematic section showing the locations of the samples obtained from the Scarborough site. The fold is outlined, and the vertically ruled unit is the upper portion of the Sunnybrook Till.

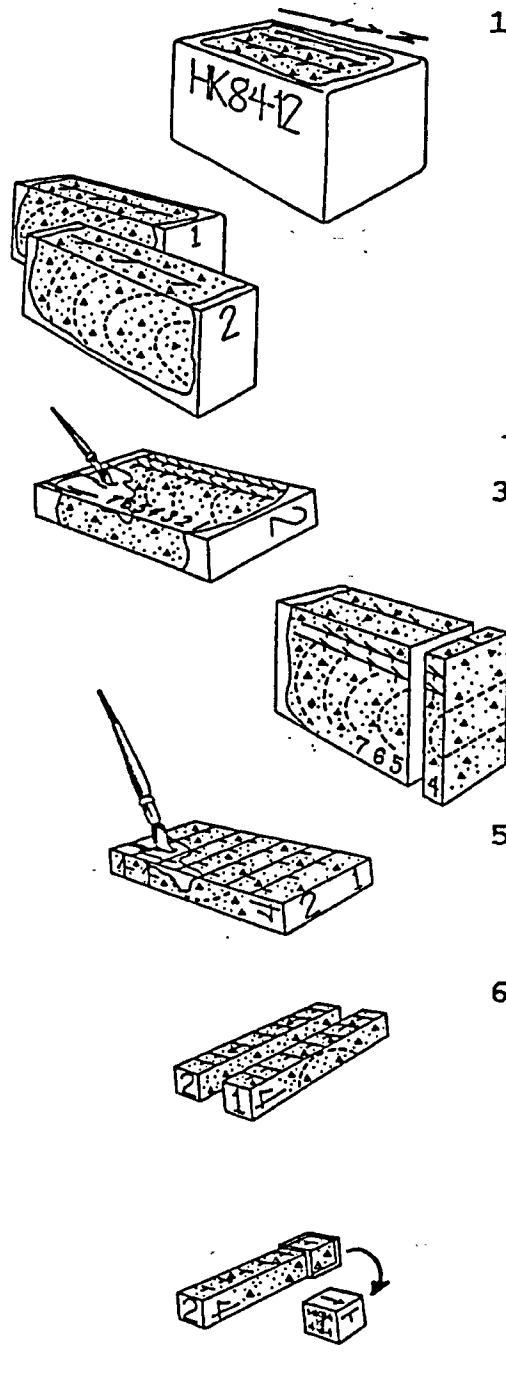
- 
1. The 15x20x20 cm field sample is set in plaster with the sides parallel to the orientation marks put on in the field
 2. The block is cut into 5 cm thick slabs perpendicular to the fold axes
 3. The exposed faces are sealed and labelled
 4. The 5 cm thick slabs are cut into 2 cm thick slabs
 5. The exposed faces are sealed and labelled
 6. The small slabs are cut into two 2x2xX cm pillars
 7. Sample containers are placed over the tops of the pillars and cut off. This is repeated until the entire pillar is consumed

Figure 2.6 Subsampling Procedure for the Hvideklint Specimens. By maintaining orientation data throughout, and by planning the cuts carefully, a complete and representative collection is obtained.

2.6 Laboratory Methods

Anisotropy of Magnetic Susceptibility:

The anisotropy of magnetic susceptibility (AMS) was determined using the Sapphire Instruments SI-2 magnetic susceptibility instrument. This device consists of an inductance coil and circuitry connected to a dedicated microcomputer. The inductance coil is placed in a double-walled Mu metal container to reduce the effect of the Earth's field and laboratory noise. When a specimen is placed in the coil the change in the inductance is recorded. Thus by measuring various orientations of the specimen the anisotropy of magnetic susceptibility (AMS) can be determined. The software which controls the instrument permits a number of methods by which the accuracy of the measurements may be enhanced. These include:

- a) Increasing the measurement time by factors of two, from one-half second up to a maximum of 8 seconds per measurement.
- b) 6, 12 or 24 measurement orientations. This allows each of the matrix elements of the AMS tensor to be measured once, twice or four times, respectively.
- c) Signal stacking, which repeats each individual measurement from 1 to n times, with a resultant increase in the signal to noise ratio of \sqrt{n} .

In all measurements, each sample measurement is bracketed by air-readings to calculate the amount of drift. The program provides a safety feature whereby the measurements must be repeated if the measured drift is too large.

The program also provides an estimate of the reliability of each measurement by computing the radius of the cone of 95% confidence (Fisher, 1953) about each of the three principal susceptibility axes. Using this estimator, the optimum combination of accuracy enhancements can be determined for each collection of specimens by repeatedly remeasuring five randomly selected test specimens from each collection using different combinations of these features. The following optimum measurement modes were determined for the two sites:

Hvideklint: 12 orientations, 8 second measure time, and no signal stacking.

Scarborough: 12 orientations, 4 second measure time, and no signal stacking.

Pebble Fabrics:

The pebble fabrics were determined by measuring the orientation of the long axes of prolate pebbles contained within the blocks. The orientations were determined by gently loosening the pebble from the matrix while preserving the mold so that the pebble can be replaced in its proper orientation. The three major axes of the pebble were measured, and if the A/B ratio was ≥ 1.7 then the

pebble was considered prolate and was replaced in its mold. A sharpened probe was then inserted into the sediment adjacent and parallel to the long axis of the pebble. The azimuthal direction (declination) in the down-dip direction and the dip (inclination) of the probe were then measured relative to the orientation reference markings which had been placed on the block in the field. Where possible, at least 50 pebble orientation measurements were taken from each of the six sample blocks.

Paleomagnetic Measurements:

The paleomagnetic remanence directions were measured using a Schonstedt SSM-1A spinner magnetometer. The natural remanent magnetisation (NRM) was determined for all samples. One representative sample from each of the seven blocks was AF step demagnetised through peak fields of 5, 10, 15, 20, 30, 40, 50 and 65 milliTesla (mT). The remaining 35 samples were bulk cleaned at 20 and 40 mT.

Mechanical Analysis:

Mechanical analyses on six samples were performed by weighing out samples containing 100 g of sediment, and then washing each sample on a screen with a passing diameter of 0.075 mm (#200 Tyler mesh). The >0.075 mm fraction was then dried at 110° C. It was then shaken through a sieve stack consisting of 4.00, 2.00, 1.00, 0.50, 0.125, and 0.075 mm screens (5, 10, 18, 36, 120, and 200 Tyler mesh).

The weight of sediment retained in each screen was then recalculated as a percentage of the total weight. The <0.075 mm fraction was placed in a 1.0 L cylinder and the volume built up to 1.0 L by the addition of triple distilled water containing a deflocculating agent (Calgon). The mixture was agitated and allowed to stand undisturbed for 2 hours and 3 minutes. At this time a 20 mL pipette was inserted to a depth of 10 cm and filled with suspensate. The 20 mL of suspensate was then dried and weighed. The weight of this residue is proportional to the weight of the fraction of the sediment particles which are $\leq 4 \mu\text{m}$ in mean diameter.

3 FIELD OBSERVATIONS AND LABORATORY RESULTS:

HVIDEKLINT SECTION

3.1 Stratigraphy

The section of the Hvideklint which was investigated is confined to the deformed assemblage on the southwest side of the main chalk allochthons which are Upper Campanian to Lower Maastrichtian in age and which comprise the Hvideklint proper. This section, 50 m wide, is made up of five distinct lithostratigraphic units (Fig. 3.1):

1. chalk;
2. laminated diamicton (deformed);
3. alluvial sands, silts, gravels (both deformed and undeformed);
4. Upper Dislocated Till; and,
5. Discordant Till.

The chalk occurs in two separate autochthonous tongues which are connected laterally to the main body of the Hvideklint chalk allochthon. The diamicton exists unconformably as a sheath around the lower chalk mass. Above and to the southwest of the chalk, stratal continuity is largely maintained within the diamicton (Fig. 3.2). This diamicton had previously been described as a glaciotectonic melange (Aber, 1980), but the stratal continuity above the chalk and an absence of exotic blocks refutes this interpretation. Examination of the section

published in Aber (1980) reveals that the portion of the section examined in the present study was largely covered with debris at that time, which has subsequently eroded. As the diamicton curves under the chalk, its character changes. First, it becomes brecciated and mixed with chalk, and then it passes through a transition into a basal zone of a mixed chalk-diamicton that is best described as a glaciotectonic microbreccia. This lower-boundary microbreccia lies unconformably upon undisturbed alluvial sands (Plates 3.1 and 3.2). The deformed alluvium to the southwest of the upper chalk tongue apparently lies conformably above the deformed diamictons. The thinner upper chalk tongue is intruded unconformably along the interface between these two sedimentary units.

The Upper Dislocated Till is the first undeformed unit to appear above the deformed sequence, and it lies unconformably above the deformed alluvium. Above the Upper Dislocated Till lies the Discordant Till, in which a thin soil profile is developed.

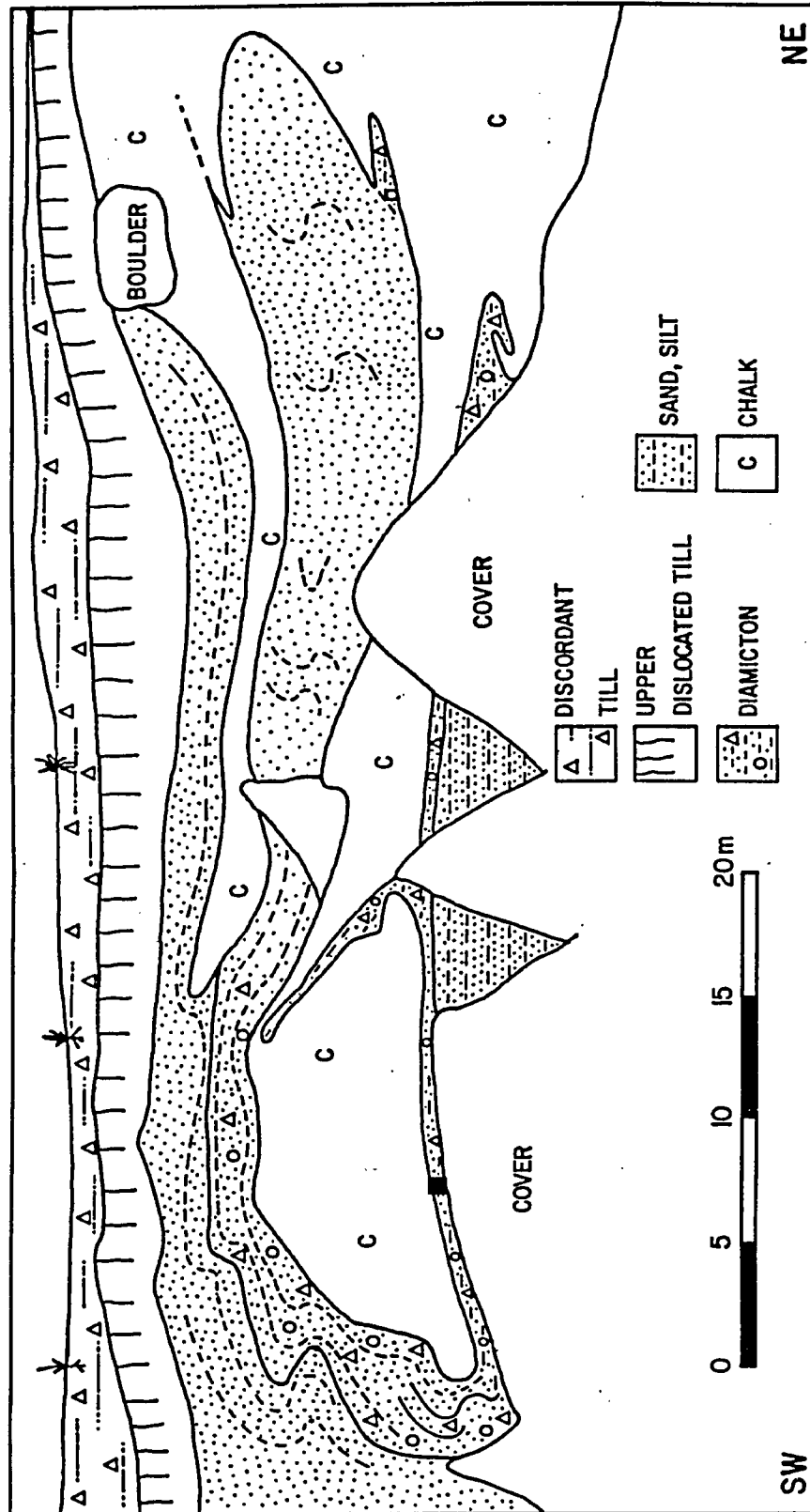


Figure 3.1 Field Sketch, Hvideklint Section
 This is a composite field sketch of the area at the southwest end of Hvideklint. The section is as viewed from the beach with minor vertical distortion. The solid square shows the location of block number HK84-09.

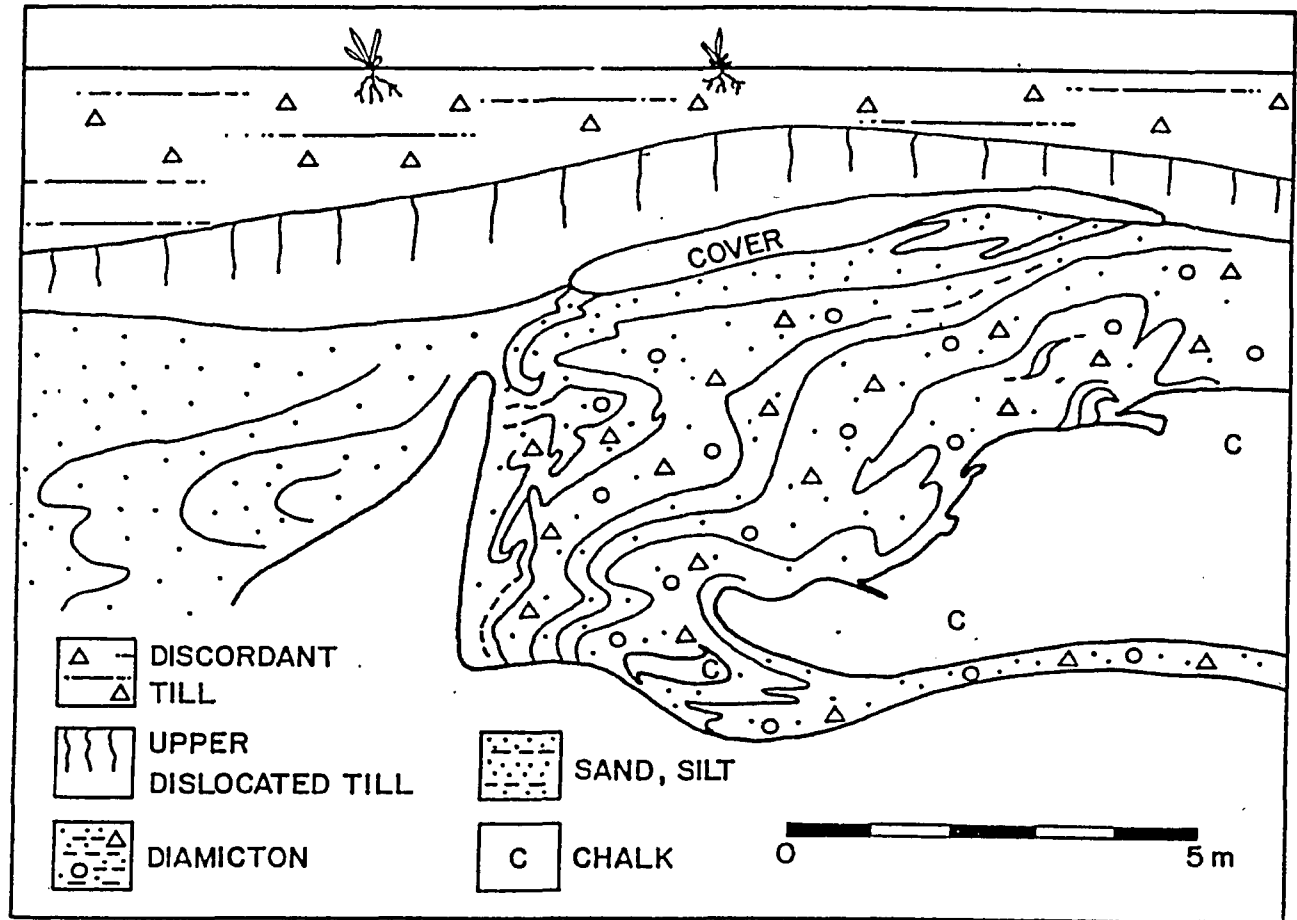


Figure 3.2 Sketch of the area immediately adjacent to the unit sampled at Hvideklint



Plate 3.1 Contact Between the Glaciotectonic Microbreccia
and Underlying Undeformed Sands.
The diameter of the lens cap is 52 mm.

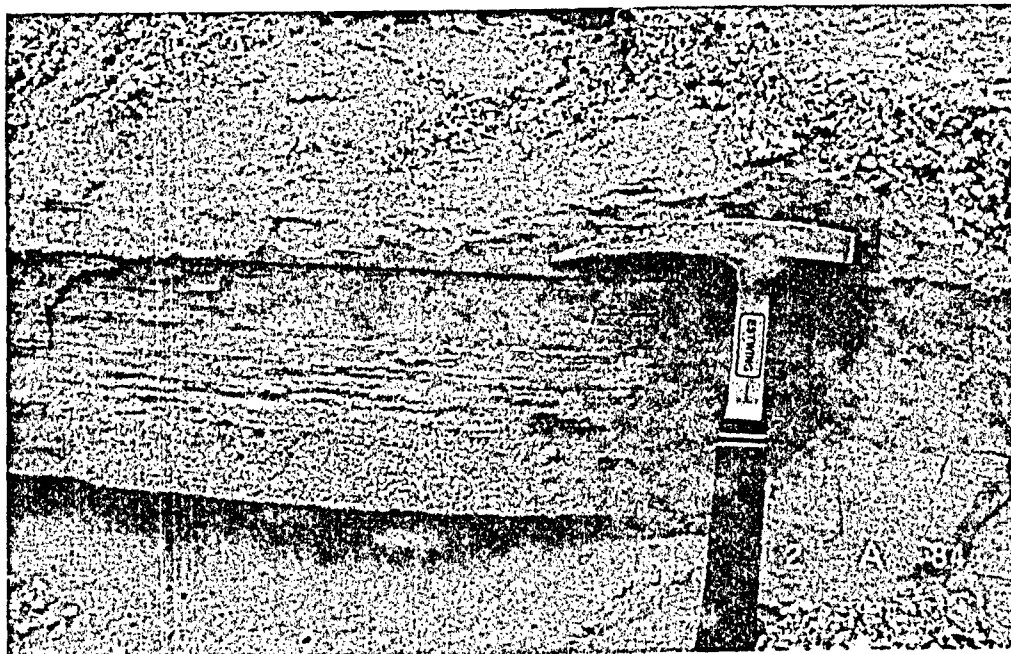


Plate 3.2 Undeformed Sands below the Glaciotectonic
Microbreccia, Hvideklint.
Hammer is 31 cm in length.

3.2 Structure

The overall structure of the deformations is that of a large, recumbent, asymmetric, non-cylindrical fold which has been displaced to the southwest along a basal shear plane. Smaller folds developed in both the diamicton and the alluvium are also overturned to recumbent, although their morphologies differ in other respects (Figs. 3.1 and 3.2). The folded unit which was sampled (Fig. 3.3) contains two recumbent, south-verging, similar folds. Despite the considerable hinge thickening of up to 100% for the lower of the two folds, the original sedimentary laminae are well preserved (Plate 3.3).

A series of small, upright, asymmetric dentations is found on the north-dipping limb (Fig. 3.3). These are interpreted as being the result of the injection of the softer, chalk-rich diamicton which is stratigraphically below, and thus are not true folds. These dentations were formed as the sediments were being compressed in that, as the inter-limb angle decreased, the diamicton in the core of the fold was injected into its neighbour. Superficially these features resemble drag folds which are caused by layer-parallel slip during progressive simple shear (Davis, 1984). Such slip is improbable for two reasons. First, the axial surface of drag folds remains perpendicular to the direction of greatest shortening. For these features to be drag folds, the direction of greatest shortening would have to be shallowly-dipping to the south. The considerable

hinge thickening of the larger-order fold negates this argument because it provides evidence for a direction of greatest shortening which is subvertical. Second, the dentations exhibit extension in their cores as shown by the distension of the thin chalky lamina and this feature supports the injection origin hypothesis (Plate 3.4). If the dentations were the result of layer-parallel slip, the outer "limbs" of the dentations would exhibit shear, not the area around the axes.

The poles to the bedding of the sampled unit and the orientation of the two fold axes are presented in Figure 3.4. At no point in the folds does the inclination (dip) of the pole to bedding exceed 60° because at all points the bedding is dipping at $\geq 30^\circ$. This is important later in considerations of the AMS and paleomagnetic results.

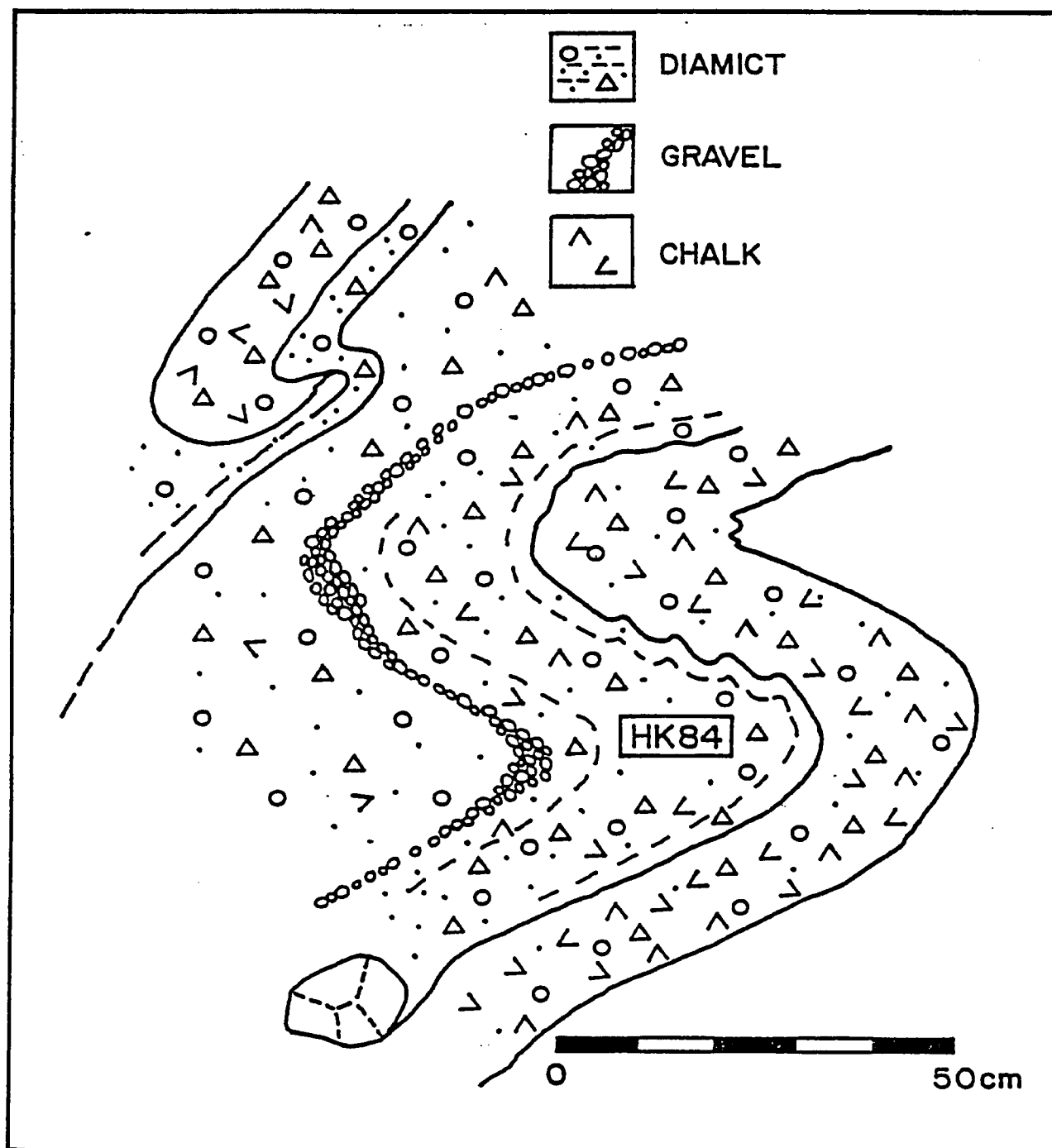


Figure 3.3 Sketch of the folded Unit, Hvideklint
 This is a detailed vertical section of the folded unit from which the HK84 samples were collected. Note that the chalk content is variable between the different beds.

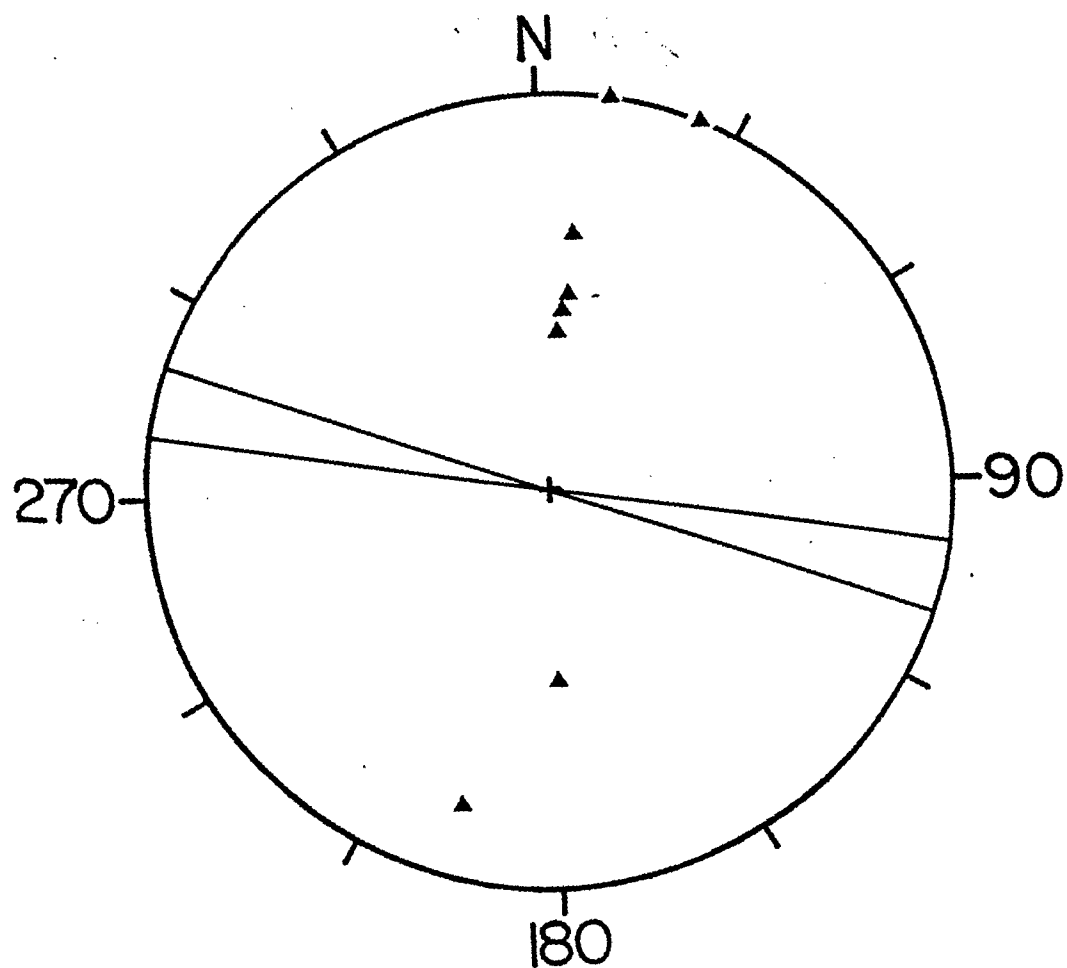


Figure 3.4 Fold Axes and Poles to Bedding, Hvideklint.
 The lines are the fold axes, and the solid triangles
 are the poles to bedding. Lower hemisphere, equal
 area (Schmidt) projection.
 Note: all stereographic representations in this thesis
 are lower hemisphere, equal area projections.

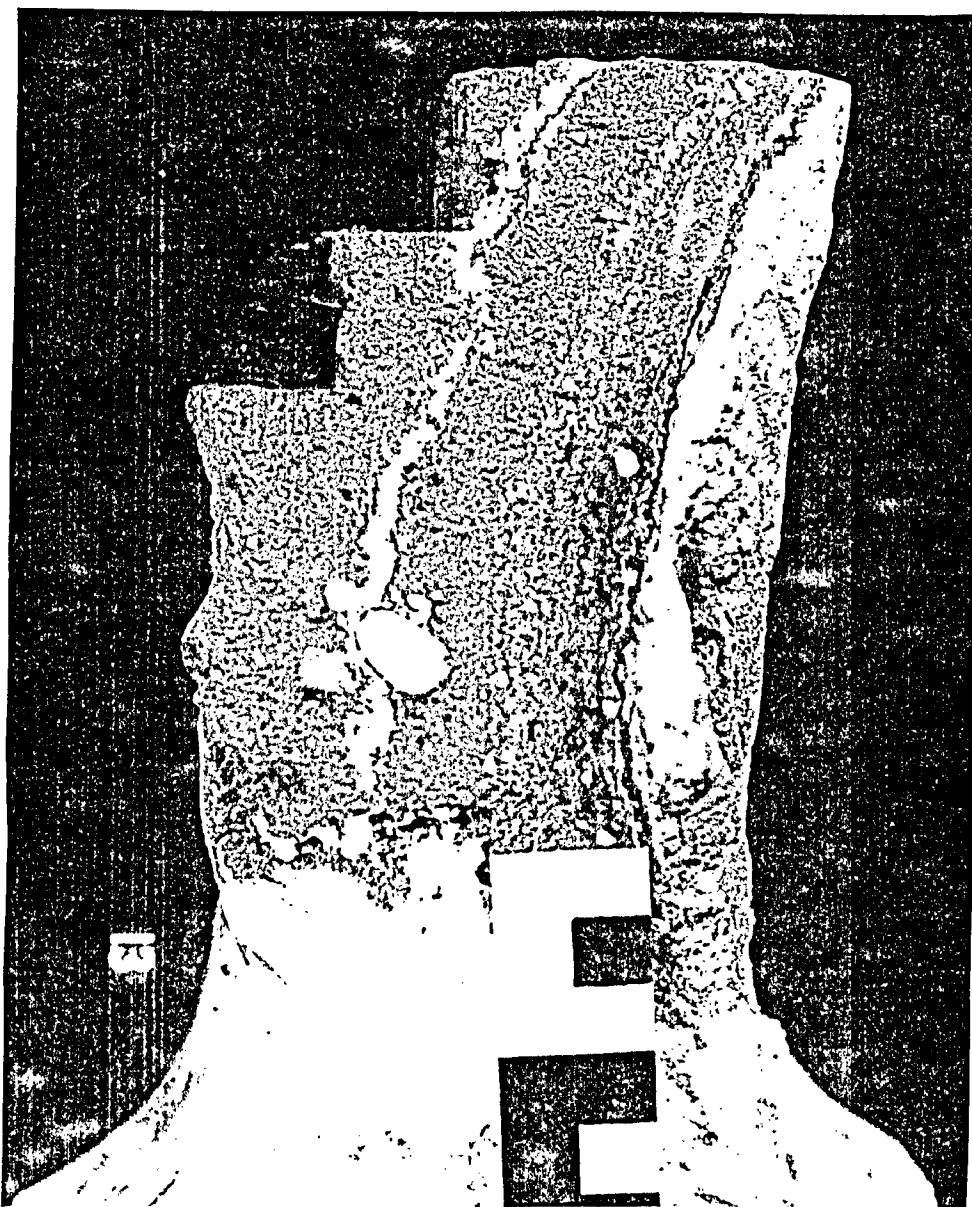


Plate 3.3 Preserved Sedimentary Lamination in Block
HK84-13, Hvideklint.
The scale is in centimetres.

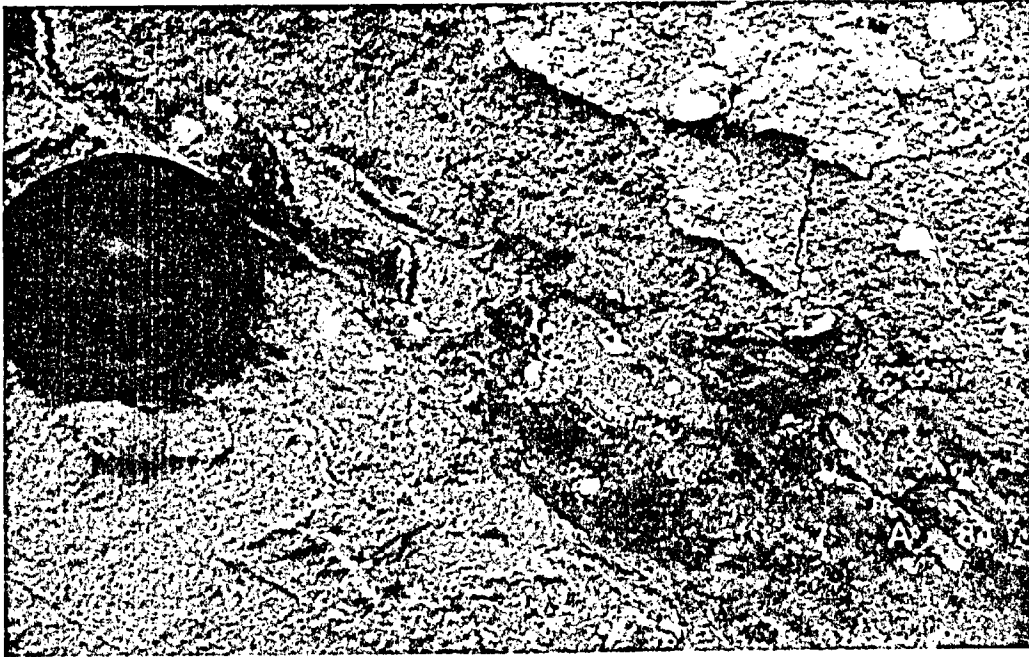


Plate 3.4 Pseudo-drag folds at Hvideklint.
Lens cap is 52 mm diameter.

3.3 Anisotropy of Magnetic Susceptibility.

The AMS was determined for 229 specimens from the Hvideklint site. The results are summarised in Table 3.1.

From the data in Table 3.1 and the contoured stereoplots of the Kmax axes (Figure 3.5), it can be seen that the mean Kmax axis remains virtually unchanged throughout the folded layer. However, while the mean Kmax axes remain constant, the patterns of their distributions vary. In the upper limb of the upper fold (Block 01), the Kmax axes exhibit a strong tendency to lie in the horizontal plane, despite the dip of the bedding. The very steeply-dipping Kmin axes (Table 3.1) have deviated from a bedding-normal position. These observations indicate that the AMS ellipsoid has been reoriented as a result of the folding. Through the fold axis and into the lower limb (Blocks 02-04), the Kmax axes are tightly clustered around the fold axis. The Kint and Kmin axes are more variable and show evidence of rotation about the fold axis. In the lower fold (Blocks 05-07) a noticeable change in the distribution of the AMS axes is seen. The Kint and Kmin susceptibility axes exhibit clustering about two respective positions whereas the tight clustering of the Kmax axes seen in the upper fold degrades to form a rough girdle in the horizontal plane (Blocks 05 and 06).

TABLE 3.1
AMS Data from Hvideklint

BLOCK	N	Kmax			Kint			Kmin		
		D	I	$\alpha 95$	D	I	$\alpha 95$	D	I	$\alpha 95$
HK84 01	28	250.5	-0.9	18.0	11.4	-61.3	19.6	46.2	78.8	20.1
HK84 02	32	265.6	10.7	13.0	7.7	41.9	18.8	176.6	63.0	16.0
HK84 03	24	264.5	4.1	7.7	357.7	61.5	13.9	174.4	27.9	13.3
HK84 04	22	272.1	3.6	19.0	14.4	38.9	23.8	187.8	50.6	16.2
HK84 05	36	286.6	4.2	13.4	18.7	15.6	15.5	182.5	73.4	10.9
HK84 06	29	276.3	3.5	17.4	24.6	9.4	19.1	177.5	77.8	9.6
HK84 07	23	274.3	9.3	19.4	357.6	-12.5	21.7	170.8	59.7	18.0
MEAN		270.0	4.1	6.0	4.8	26.4	7.7	175.7	65.4	6.0
HK84 09	35	291.3	-4.1	12.2	20.4	11.1	12.4	37.5	-77.1	3.9

Notes:

N = number of specimens

D = declination (azimuth) (degrees)

I = inclination (dip) (degrees)

 $\alpha 95$ from Fisher, 1953 (degrees)

This pattern continues into the lowermost limb (Block 07) with only minor modification. There is again no relationship between the AMS and the attitude of the bedding (Blocks 04-07). These data suggest that there is an obvious change in the state of strain between the upper and lower folds.

The fabric parameters also exhibit variations through the folded sequence (Table 3.2). The ellipticity ("E") parameter shows that the magnetic fabric is initially oblate in shape, constricts to a prolate shape through the upper fold hinge, and then returns to an oblate shape in the lower fold. This pattern of magnetic fabric variation is consistent with the distribution of the principal susceptibility axes described above. In an oblate ellipsoid the K_{max} and K_{int} axes may fluctuate within their plane while the K_{min} axis remains "fixed". In a prolate ellipsoid, just the opposite is possible with the K_{max} axis "fixed" while K_{int} and K_{min} fluctuate in a plane normal to K_{max} . These are the same the relationships which are observed between the principal susceptibility directions and the ellipsoid shape.

The parameter "Q" is often used as an estimator of the overall shape of the AMS ellipsoid. However, in comparison with the ellipticity parameter, "Q" is clearly deficient in one important respect, ie., in "E" the oblate-prolate transition lies precisely at the value 1.000 whereas with "Q" there is no clearly defined fabric shape

transition. Several researchers (e.g. Hamilton and Rees, 1970; Gravenor, 1985a) use "Q" as an indicator of whether or not the sediment has undergone postdepositional deformation. A "Q" value of 0.67 or greater is supposed to indicate that the sediment has been deformed or deposited on a paleoslope (Hamilton and Rees, 1970). Analysis of Table 3.2 indicates that to use "Q" as an indicator of deformation is clearly invalid. The portions of the fold which exhibit the greatest deformation also exhibit the smallest "Q" values which are less than 0.67. Furthermore, there is no simple linear relationship between "E" and "Q", so the value of "Q" as an estimator of the true shape of the ellipsoid is also questionable. For these reasons the "Q" parameter cannot be reliably used in the interpretation of deformed sediments.

The AMS in the lower boundary microbreccia (Block 09) does not differ greatly from the AMS through the folds in terms of the orientation of the three principal susceptibility axes (Figure 3.6, Table 3.1). The shape of the ellipsoid is different, however. The AMS ellipsoid in the glaciotectonic microbreccia is more prolate (Table 3.2) thus having the highest ellipticity, a high value for the foliation and a low lineation. It is again worth noting that "Q" is remarkably low despite the fact that this portion of the sequence is arguably the most strongly deformed.

TABLE 3.2

AMS Fabric Data from Hvideklint.

BLOCK	N	<u>LINEATION</u>		<u>FOLIATION</u>		<u>Q</u>		<u>E</u>	
No.		Mean	SD	Mean	SD	Mean	SD	Mean	SD
HK84 01	28	3.82	±2.93	5.96	±4.71	.766	±.430	1.005	±.048
HK84 02	32	3.58	2.38	4.77	2.39	.795	.423	0.995	.034
HK84 03	24	3.48	3.33	4.76	4.49	.771	.331	0.997	.019
HK84 04	22	4.00	3.62	8.14	7.67	.579	.338	1.027	.048
HK84 05	36	3.48	4.90	6.29	4.88	.487	.365	1.014	.050
HK84 06	29	3.57	5.98	6.92	11.21	.500	.264	1.026	.082
HK84 07	23	4.34	3.49	6.43	5.06	.685	.354	1.002	.028
HK84 09	35	2.63	2.23	6.74	2.13	.373	.233	1.030	.026

Lineation, Foliation, Q, and E are defined in the text.

SD is the Standard Deviation.

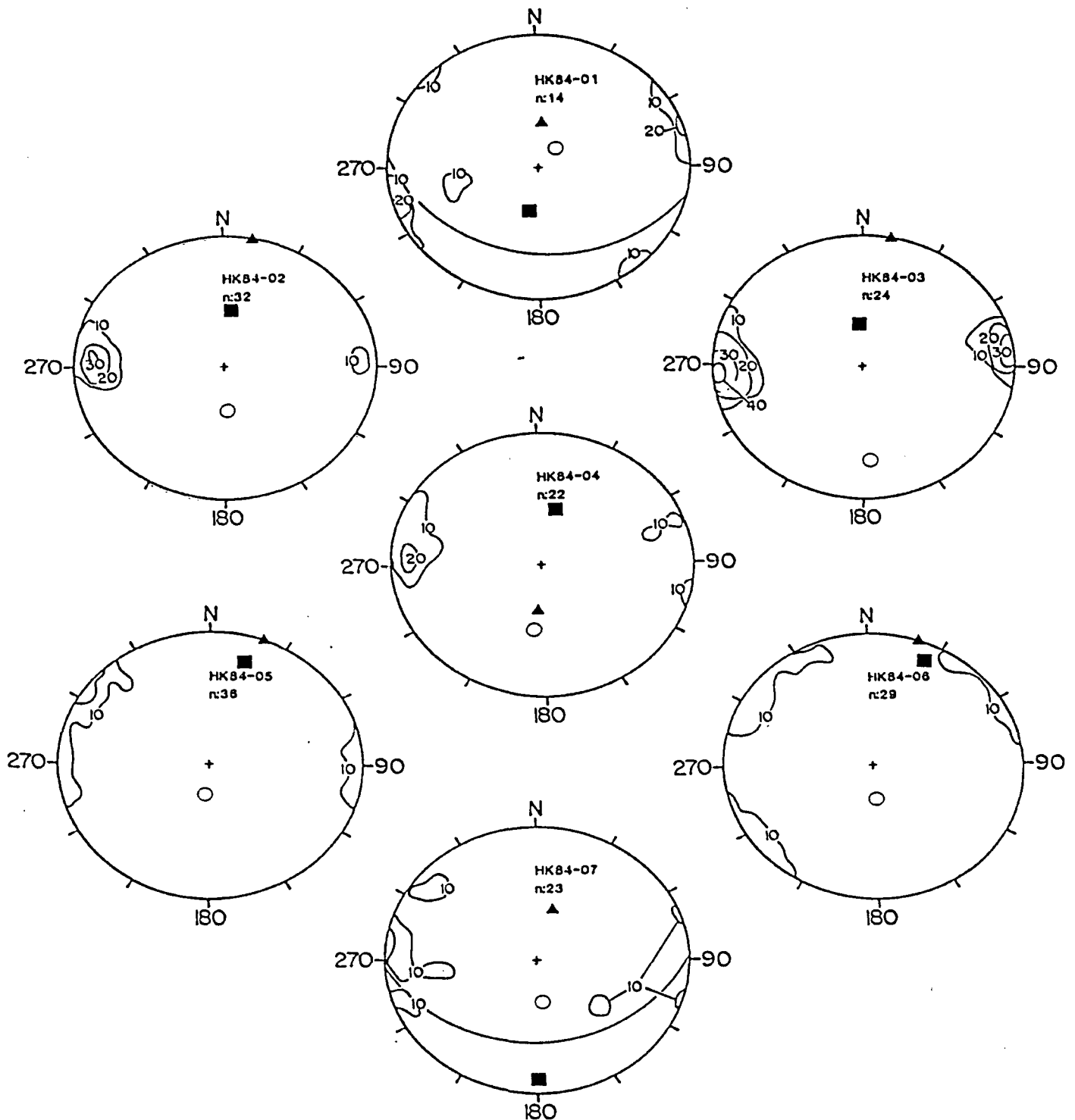


Figure 3.5 Stereoplots of Kmax Directions, Hvideklint.
Area of smoothing circle: 2%. Contour interval in per-cent.

▲: poles to bedding Great circles: bedding
○: mean Kmin directions ■: mean Kint directions

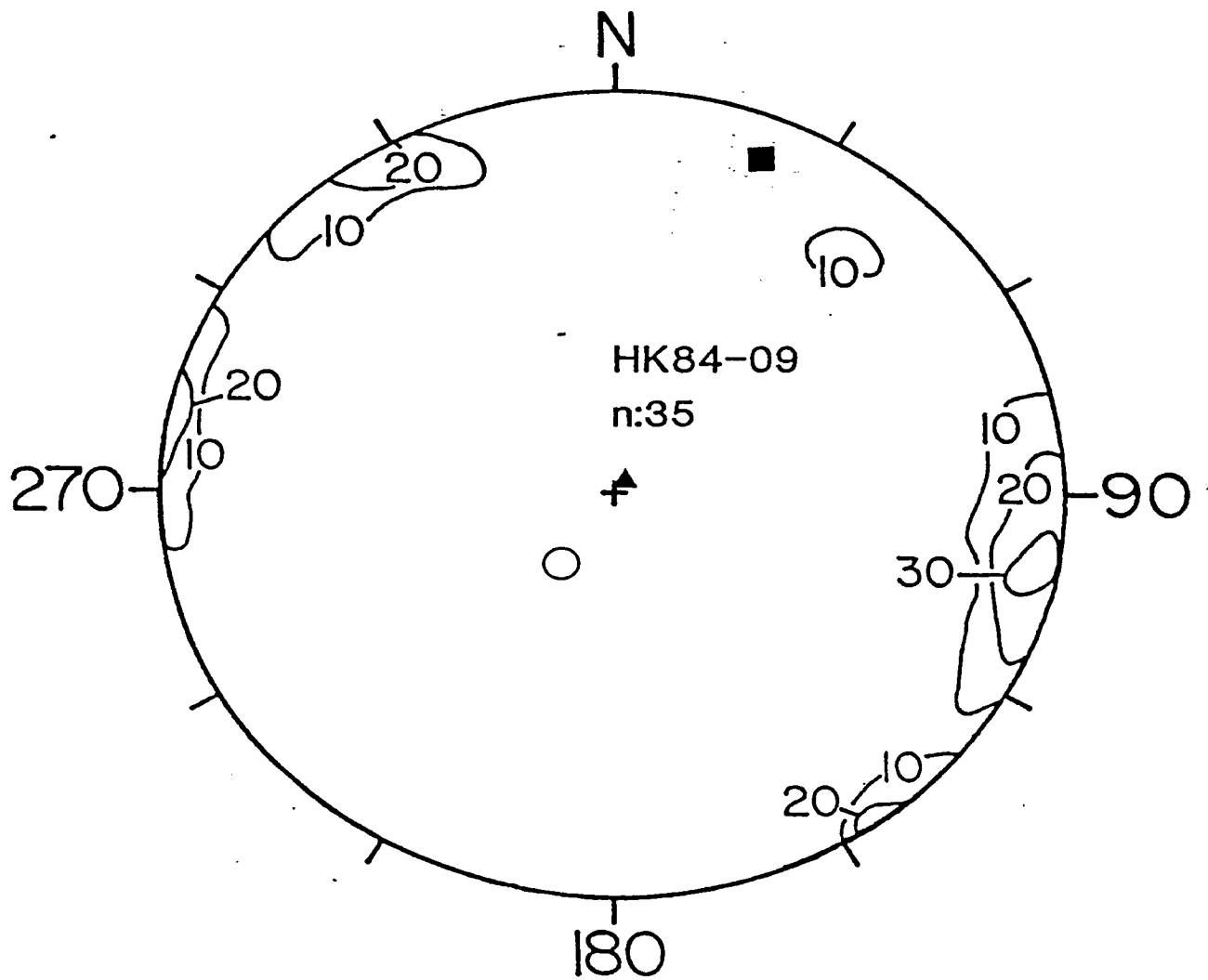


Figure 3.6 Stereoplot of Kmax directions, Block HK84-09.
Legend as in Figure 3.5.

3.4 Pebble Fabrics

Analysis of the clast fabric data (Figure 3.7) reveals that the mesofabrics of the sediments are not as easily reoriented as the magnetic fabrics, although the mean directions are consistent throughout (Table 3.3). In the uppermost and lowermost limbs there is an obvious tendency for the long axes of the prolate pebbles to lie within the original bedding plane. Through the fold hinges and the shared central limb the pebbles, like the AMS, have been strongly affected by the strain. The distribution of the pebble axis directions is also similar in pattern to that of the Kmax directions of the AMS. The orientations of the "A" axes of the pebbles exhibit a tight clustering about the fold axis in the upper fold (Blocks 12 and 13), but in the lower fold (Block 16) the long axes of the pebbles show a distribution within the horizontal plane.

TABLE 3.3

Pebble Fabric Data from Hvideklint

Block Number	Number of Pebbles	Mean Declination	Mean Inclination	α_{95}
HK84 11	50	249.9	-15.1	11.5
HK84 12	50	279.7	19.0	9.7
HK84 13	44	277.4	- 1.0	10.9
HK84 14	23	248.5	5.3	10.1
HK84 16	45	277.4	11.3	9.2
HK84 17	50	279.8	4.2	11.2

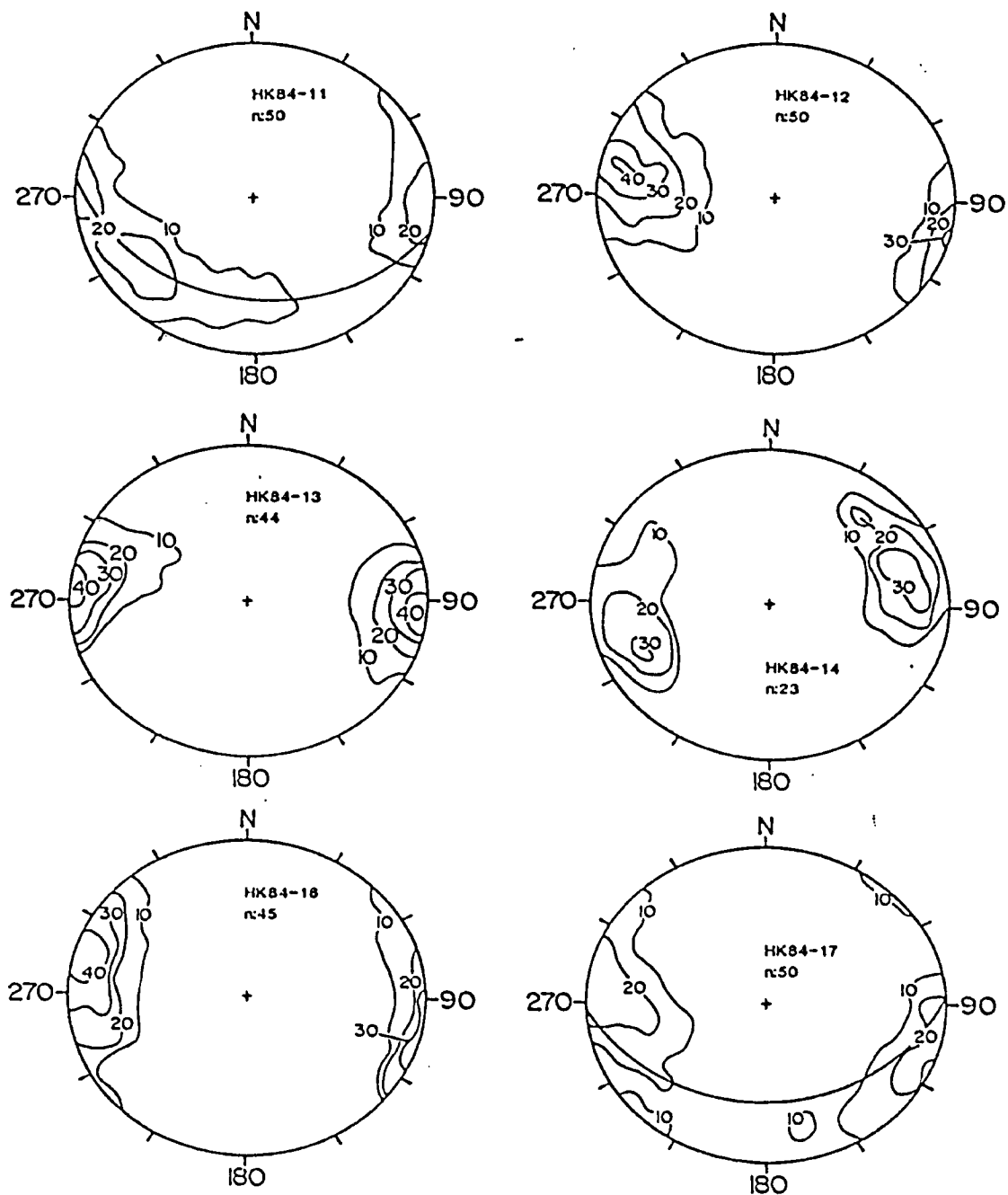


Figure 3.7 Pebble Orientations, Hvideklint.
Smoothed stereoplots of the orientations of the long axes of prolate pebbles for each of the blocks in the collection. Contour interval is in per-cent. The area of the smoothing circle is 5%.

3.5 Paleomagnetism

Step demagnetisation of the seven pilot specimens (Figure 3.8) reveals a progressive and fairly coherent demagnetisation behaviour of the specimens after 10-20 mT and up to 50 mT, at which point samples 01 and 04 begin to behave erratically. This pattern of demagnetisation suggests that the specimens record stable paleomagnetic directions in the 20 to 50 mT range of demagnetisation. All of the viscous remanence component appears to be removed by 20 mT and therefore bulk demagnetisation values of 20 and 40 mT were selected. Analysis of the directional data (Figure 3.9) reveals significant scattering of the actual directions at both 20 and 40 mT. At 40 mT the only pattern evident is a crude deviation of the paleomagnetic vectors away from the fold axes. Analysis of the block mean directions (Figure 3.10, Table 3.4) demonstrates that the remanence directions do not record the prefolding direction, because:

- i) blocks 01 and 07 have similar bedding orientations yet there is no clustering of remanence directions;
- ii) the directions from the two blocks from each fold axis should cluster yet blocks 02 and 03, and blocks 05 and 06 have mean directions which differ by as much as 70°; and,
- iii) the mean directions from all seven blocks should lie on a single small circle about the fold axes and they do not.

It is difficult to interpret data which are simultaneously both magnetically stable and directionally scattered. The only reasonable interpretation is that the primary remanence was in part reset and in part rotated during deformation. The remanence was unable to align with the paleofield due to the simultaneous reorientation of both the meso- and magnetic-fabrics with the stress field. The remanence directions could have been affected also by possible eddying in the sediment as the larger sand- and pebble-sized particles were physically reoriented in response to the applied stress.

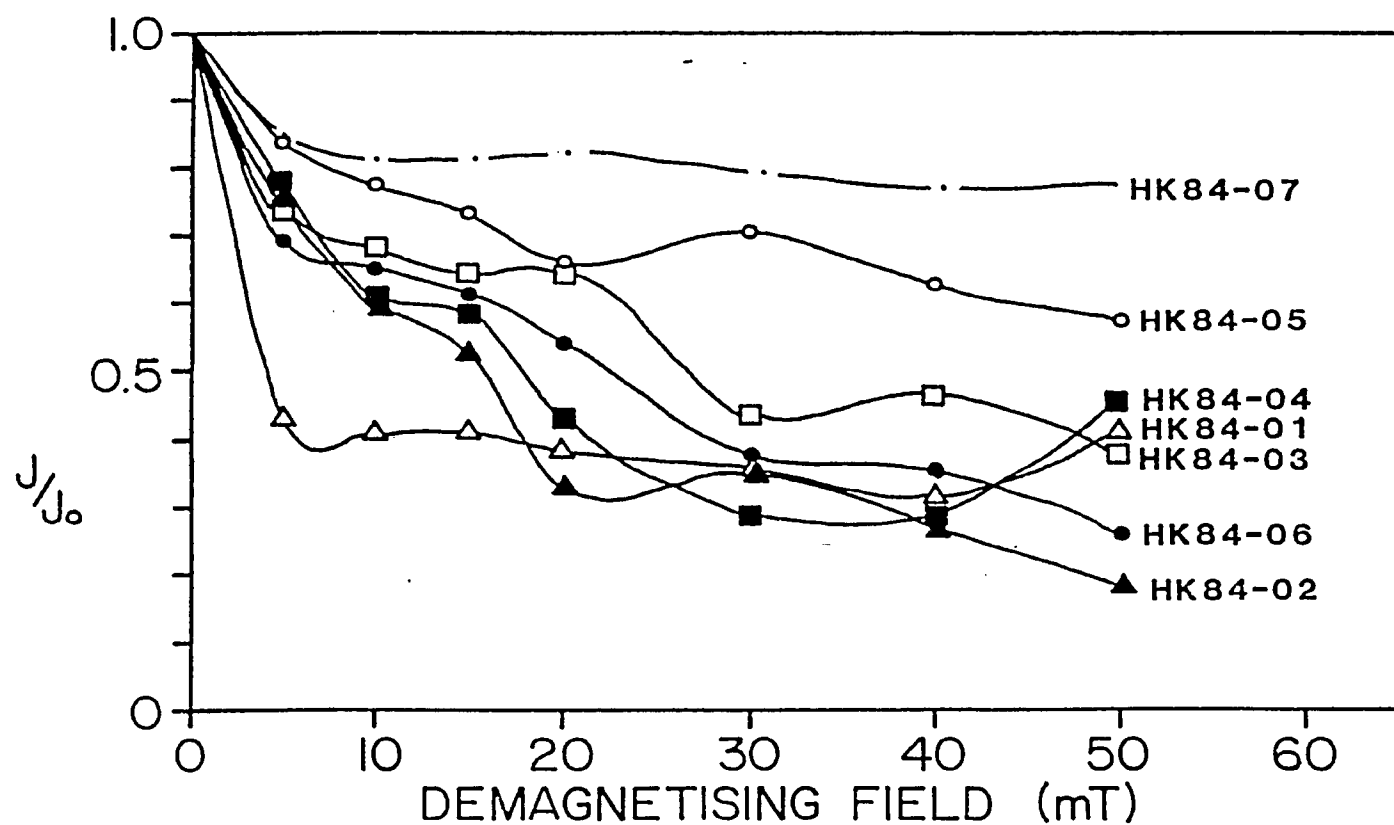


Figure 3.8 Step Demagnetisation Data, Hvideklint.
 J/J_0 is the change in intensity of magnetisation relative to the strength of the NRM for each specimen.

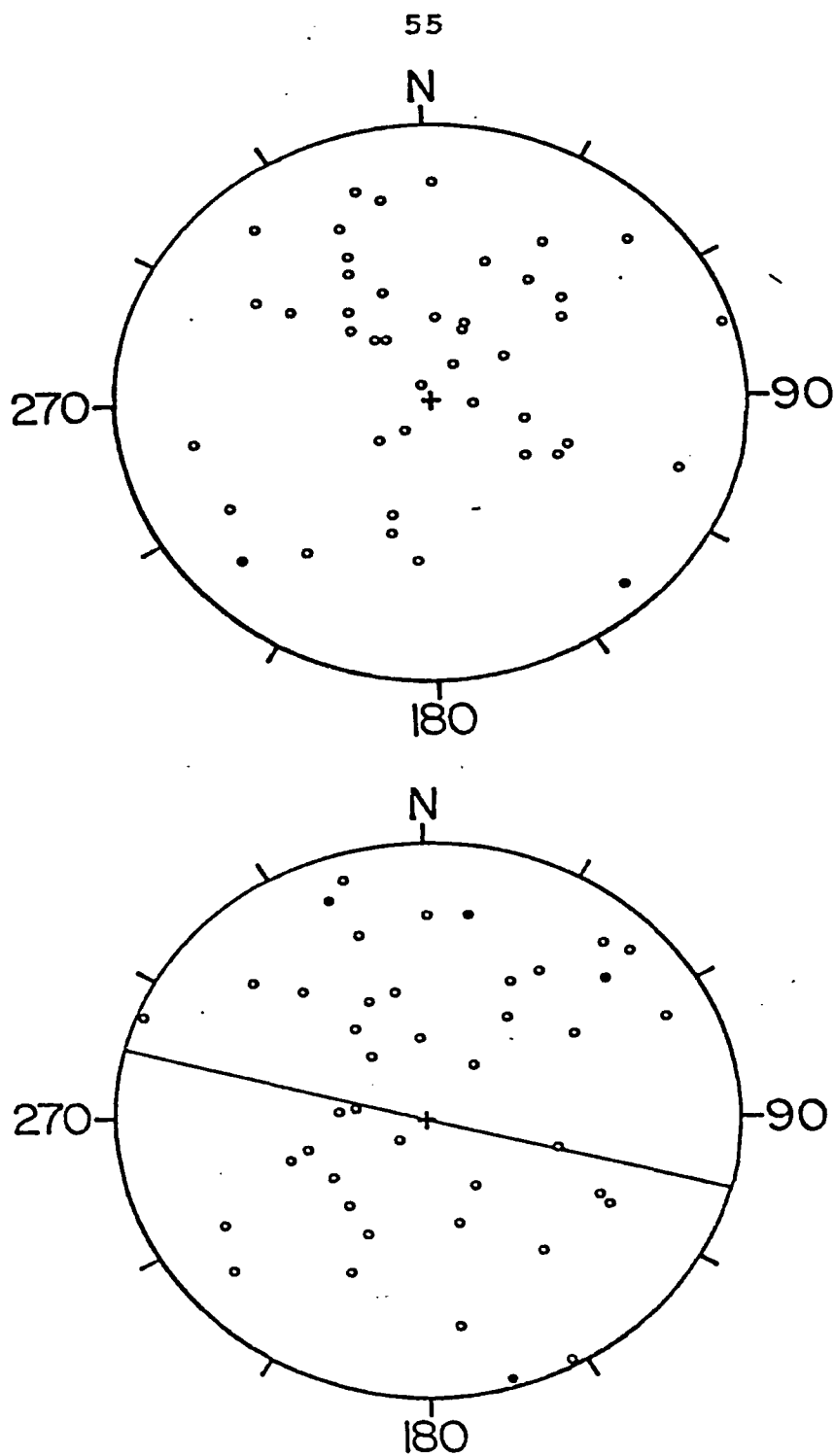


Figure 3.9 Remanence Directions, Hvideklint.
 Top: 20 mT Bottom: 40 mT Line: mean fold axis
 Open circles represent down directions, closed circles
 are up directions.

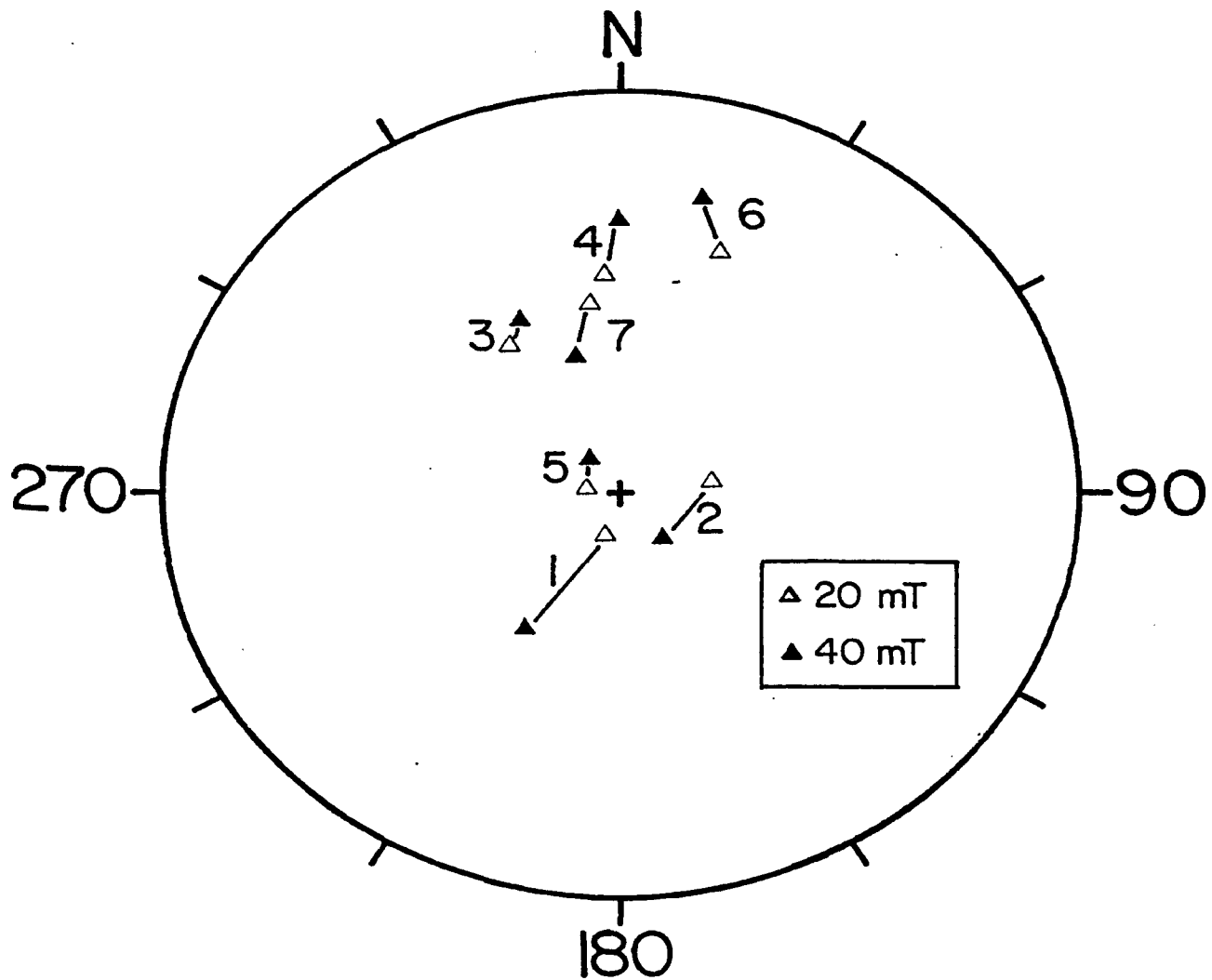


Figure 3.10 Block Mean Remanence Directions.
All directions are down directions.

Table 3.4
Block Mean Remanence Data for Hvideklint

Block Number	Number of Specimens	Mean Declination	Mean Inclination	α_{95}
---20 mT---				
HK84 01	6	192.1	81.4	38.0
HK84 02	6	82.5	73.8	32.8
HK84 03	6	323.9	55.1	42.5
HK84 04	6	355.1	48.5	28.2
HK84 05	6	273.8	83.3	45.8
HK84 06	6	19.3	41.0	39.9
HK84 07	6	351.2	53.4	49.3
HK84 09	6	18.4	46.1	28.6
---40 mT---				
HK84 01	6	210.0	59.3	27.7
HK84 02	6	145.9	79.1	49.8
HK84 03	6	330.9	53.1	46.3
HK84 04	6	358.6	36.3	47.3
HK84 05	6	316.4	81.8	49.4
HK84 06	6	13.6	31.6	41.9
HK84 07	6	343.1	62.2	47.2
HK84 09	6	77.8	16.2	47.3

3.6 Mechanical Analysis

The sediment samples exhibit poor sorting with a bimodal distribution of grain sizes and therefore the sediment can be classified as a diamicton (Figure 3.11). Using the simplified nomenclature of Wentworth (1922), this sediment is a 'clayey-sand'. A pebble count (Figure 3.12) shows that the pebbles in this sediment are predominantly sedimentary and igneous in origin along with significant percentages of chalk and flint. This distribution differs from those described by Aber (1980) for the till units of Hvideklint in that the chalk component is noticeably lower i.e. 15% versus 30-50% in the tills.

Analysis of the variation in the total carbonate content, as estimated by the acid soluble fraction (Figure 3.13), reveals that there is a significantly larger proportion of carbonate material in the silt and clay size ranges. This can be accounted for in two ways. First, chalk is composed of the tests of microscopic foraminifera and nannofossils. When the chalk disaggregates, those tests, both whole and broken, would be included in the resulting sediment. Second, the glaciotectionic folding of the sediment could further crush the tests thereby increasing the carbonate content in the silt and clay size ranges.

The poorly-sorted texture, well-developed lamination, presence of interbedded water-washed gravels and sands, and the conformity with the outwash sands and silts which lie

stratigraphically above indicate that the sediment sampled at Hvideklint is the product of subaqueous mass flow.

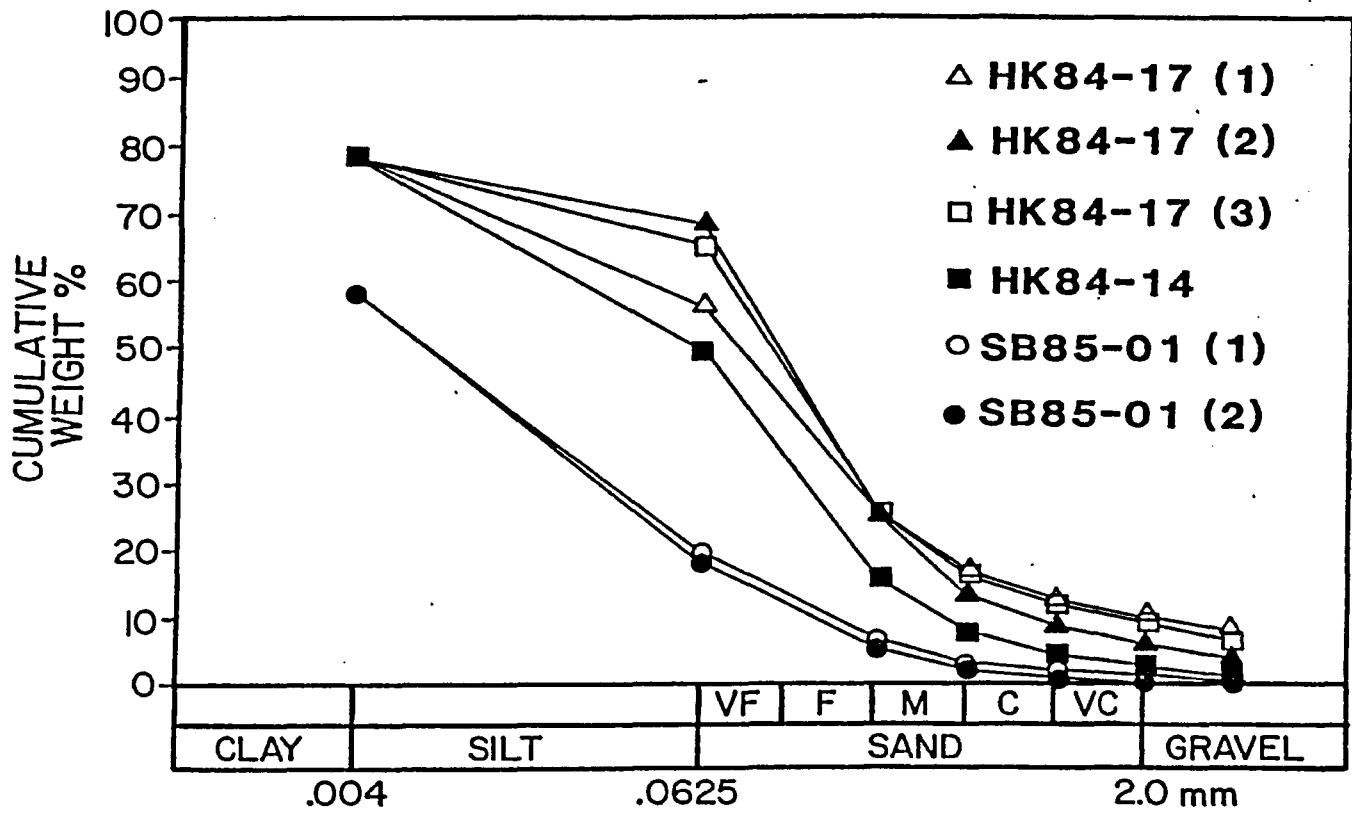


Figure 3.11 Grain Size Distributions.
The scale used is that of Wentworth (1922).

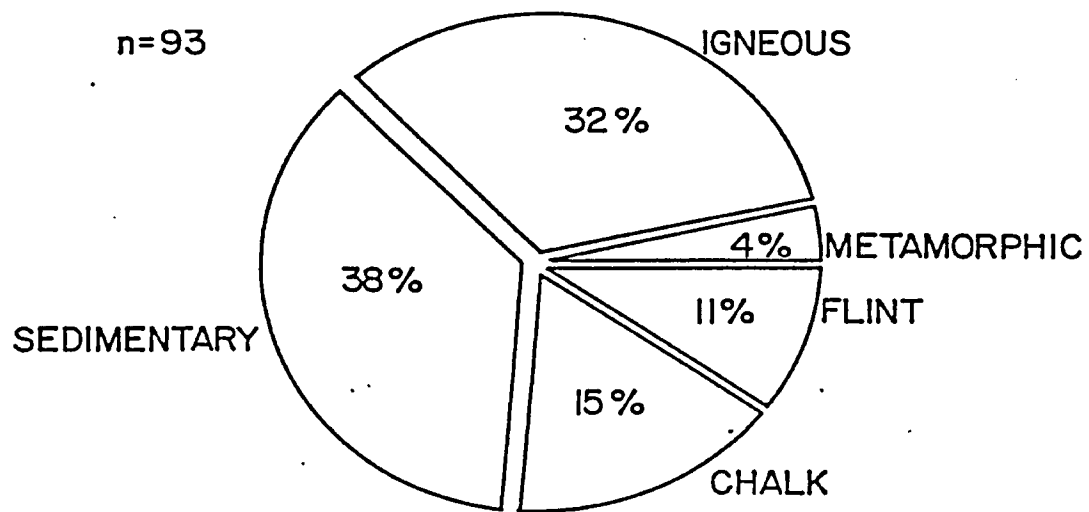


Figure 3.12 Pebble Lithologies from Block HK84 14,
Hvideklint.

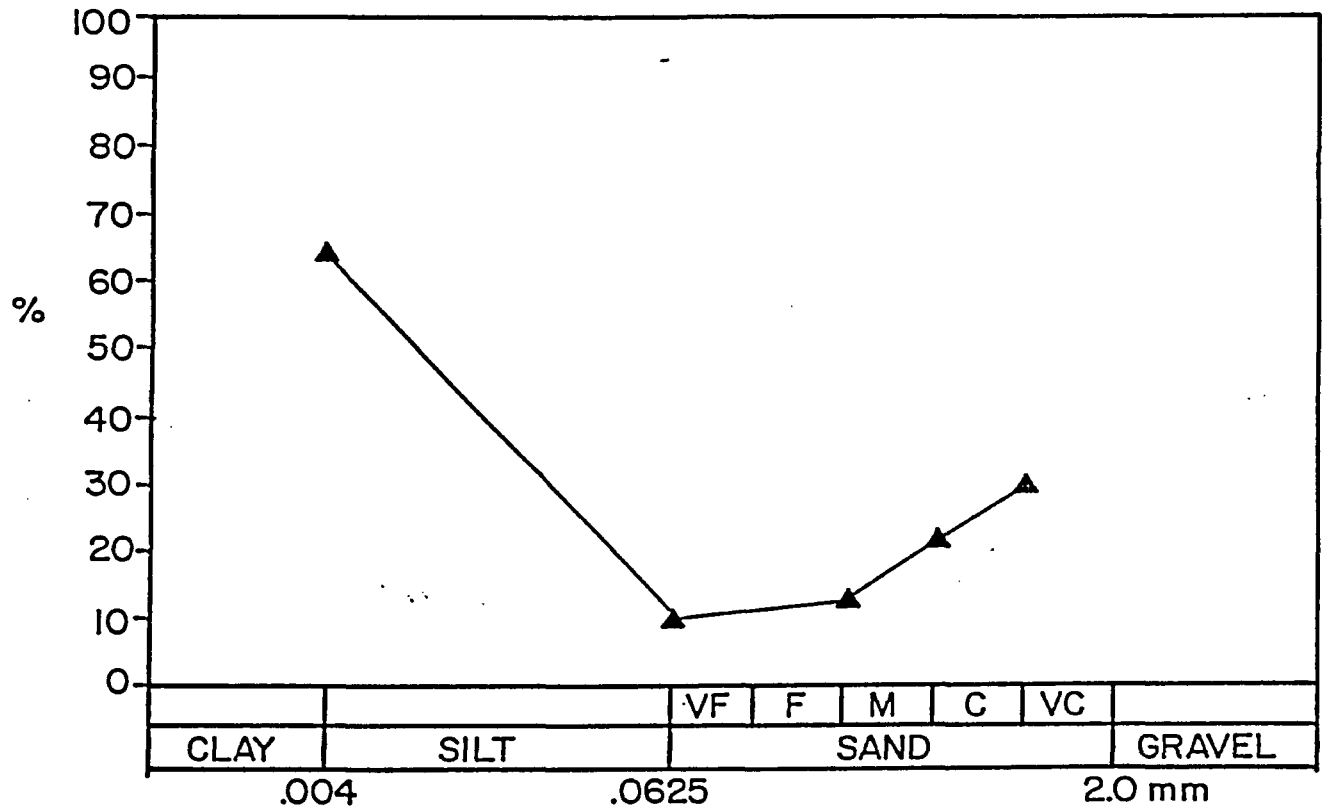


Figure 3.13 Carbonate Content of Block HK84 14,
Hvideklint.

SCARBOROUGH SECTION

3.7 Anisotropy of Magnetic Susceptibility

The directional data for the AMS results from the Scarborough section are given in Table 3.5. The fabric data are given in Table 3.6. The fold axis is oriented N10°W and the direction of flow is inferred to have been from the ENE. As can be seen from Table 3.5, the AMS ellipsoid maintains a constant orientation throughout the fold with Kmax closely parallel to the orientation of the fold axis. The distribution of the principal susceptibility axes (Figure 3.14) shows that Kmax and Kint axes are slightly scattered in a plane dipping at approximately 10° NNW. The Kmin axes are circularly clustered about a mean direction.

The shape of the susceptibility ellipsoid exhibits a spatial variation within the flow fold. The upper and foremost block (Block 01, Figure 2.5) in the downstream direction possesses the lowest value of ellipticity, and the lowermost block (Block 06) the greatest. If the blocks are traced in succession around the fold, following the original sedimentary layering, it can be seen that the ellipsoid shape varies systematically. Initially (Block 04) the ellipsoid is moderately prolate with an ellipticity of 1.022. As the sediment approaches the fold hinge, the ellipticity decreases through 1.011 in block 03

to a minimum of 1.009 in block 01. In the hinge area itself, the ellipticity begins to increase to 1.023 in block 02 and by the time the sediment reaches the base of the flow fold (Block 06) the ellipticity has increased to a maximum of 1.034. The central portion of the fold (Block 05) possesses a mean ellipticity value of 1.021, which is intermediate. However, the core of the fold (Plate 3.5) also exhibits a distribution of fabric shapes similar to that observed in the entire fold (Figure 3.15). The exception is that the lower limb does not exhibit flattening at the base, but rather in the hinge area of the fold.

TABLE 3.5
AMS Data from Scarborough

BLOCK	N	Kmax			Kint			Kmin		
		D	I	$\alpha 95$	D	I	$\alpha 95$	D	I	$\alpha 95$
SB85 01	21	335.3	14.9	14.3	65.7	4.4	14.8	343.1	-74.5	4.7
SB85 02	20	337.4	8.1	3.9	69.4	15.6	5.5	38.0	-71.4	4.9
SB85 03	20	330.8	18.9	5.5	60.0	-3.7	6.1	319.2	-71.9	3.9
SB85 04	27	320.1	12.2	4.9	50.3	0.4	4.7	320.3	-77.6	2.9
SB85 05	62	339.5	8.3	6.1	69.2	2.3	5.8	348.0	-80.4	3.3
SB85 06	27	310.1	10.2	10.9	44.5	17.8	11.0	10.1	-69.8	3.2
SB85 07	23	340.7	11.7	9.9	70.5	6.5	8.7	3.1	-76.5	6.3

Note: The legend is the same as in Table 3.1

Table 3.6
AMS Fabric Data from Scarborough.

<u>BLOCK</u>	<u>LINEATION</u>		<u>FOLIATION</u>		<u>"Q"</u>		<u>"E"</u>	
<u>NUMBER</u>	Mean	SD	Mean	SD	Mean	SD	Mean	SD
SB85 01	3.97	±2.06	6.65	±1.33	.578	±.277	1.009	±.024
SB85 02	5.40	1.11	9.99	1.46	.543	.090	1.023	.015
SB85 03	4.48	1.45	7.58	0.58	.592	.193	1.011	.021
SB85 04	3.93	1.40	7.87	2.20	.512	.187	1.022	.027
SB85 05	4.04	1.82	7.93	2.70	.520	.201	1.021	.023
SB85 06	0.78	0.37	4.48	0.74	.174	.086	1.034	.008
SB85 07	4.52	2.39	8.34	1.71	.547	.293	1.019	.036

SD is Standard Deviation

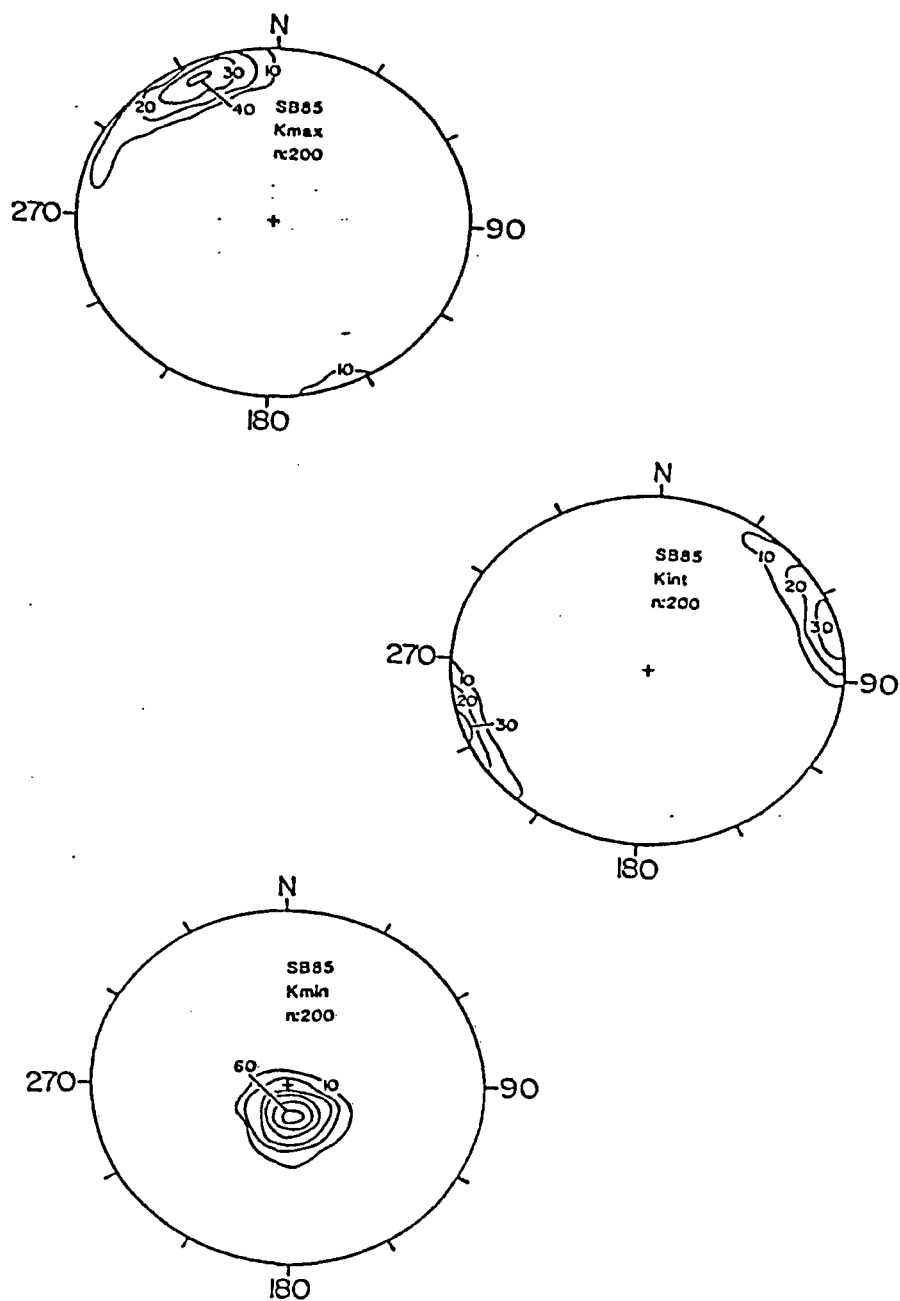


Figure 3.14 Stereoplots of Principal Susceptibility Directions, Scarborough.
Area of smoothing circle is 2%, contour interval is in percent.

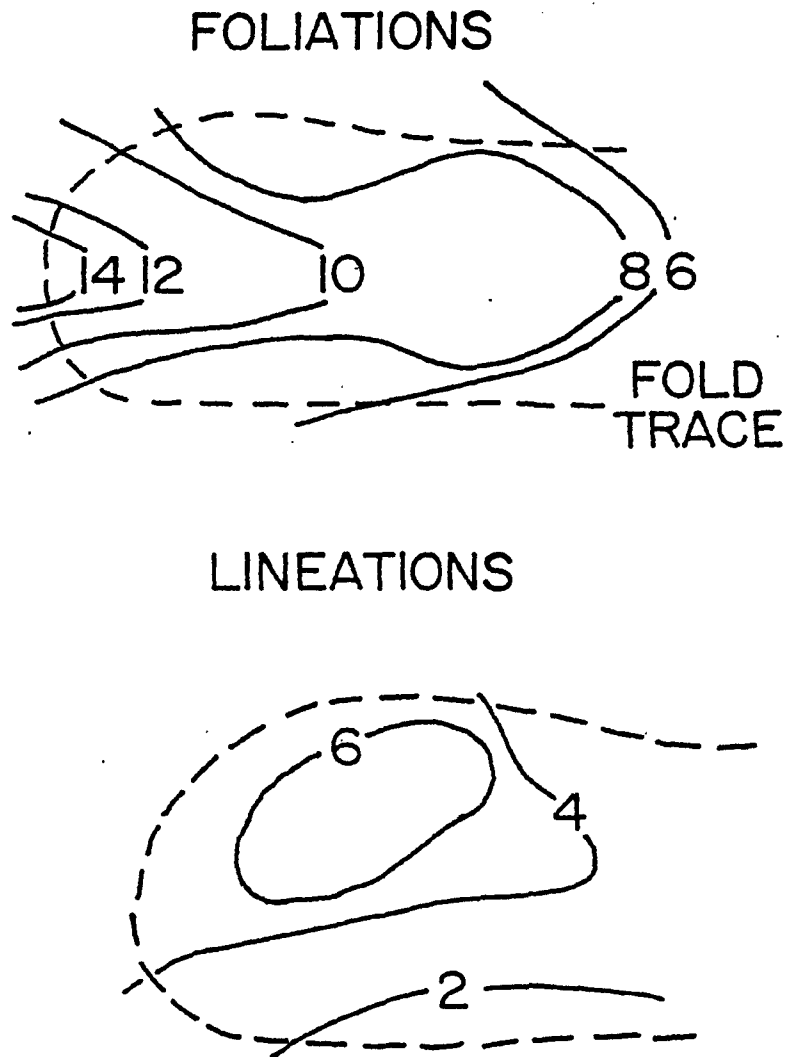


Figure 3.15 Distribution of AMS Ellipsoid Shapes in Block SB85-05.

The spatial variation in ellipsoid shape is demonstrated using the parameters of lineation and foliation. The section is normal to the fold axis. The units of lineation and foliation are percent.

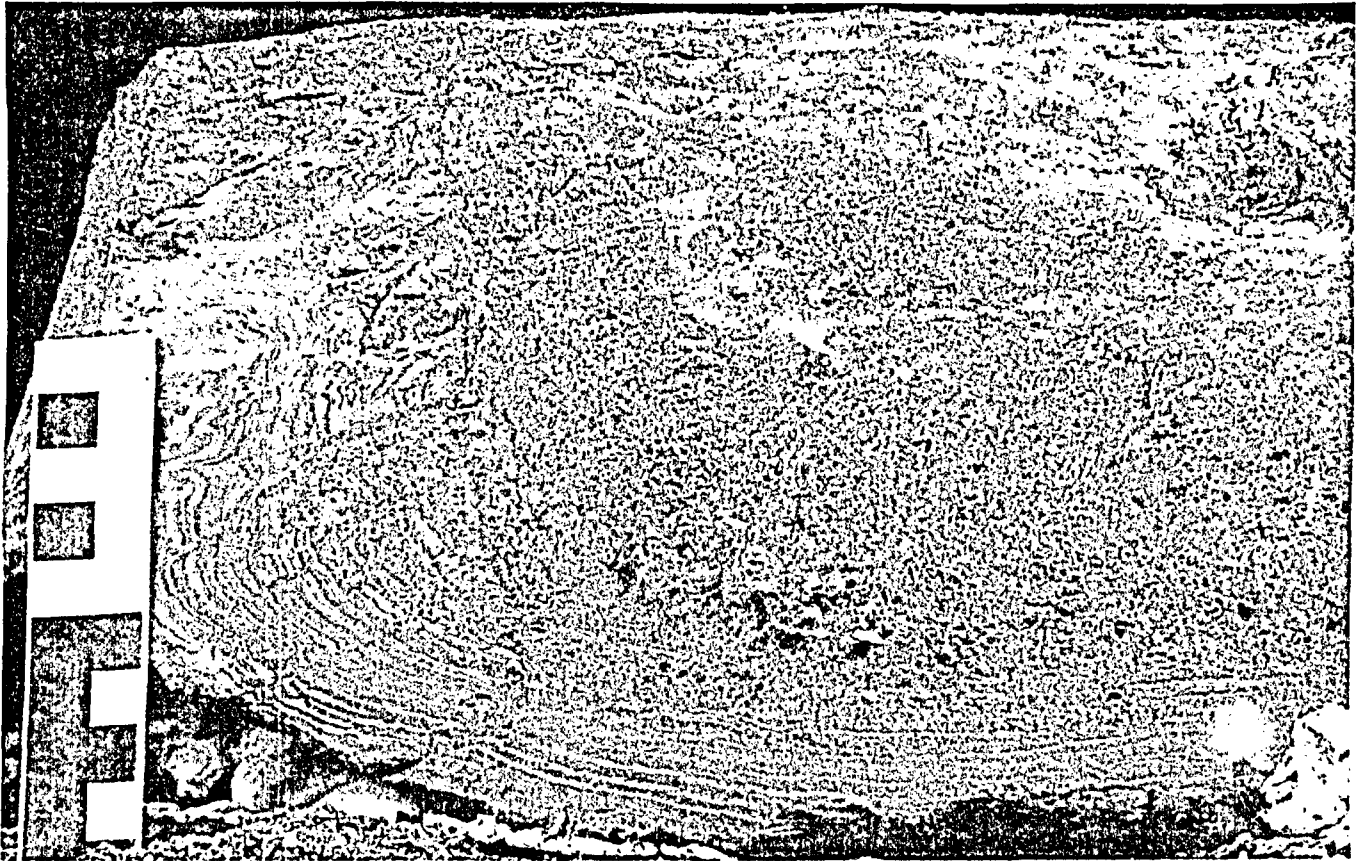


Plate 3.5 Centre of the Scarborough Flow Fold.

Block number 05. The scale is in centimetres. The photograph is at right angles to the fold axis, and a layer of unconsolidated sand can be seen to be continuous along the lower limb of the fold and through the hinge of the fold. The original sedimentary laminae are preserved, and microfolding is seen in the hinge area.

3.8 Mechanical Analysis

Two mechanical analyses of the sediment sampled at Scarborough (Figure 3.11) show that they are poorly-sorted silty clays. At 0.5%, the extremely low content of clasts greater than 2 mm in diameter precluded performing pebble fabric or composition analyses.

4 INTERPRETATION OF THE HVIDEKLINT SECTION

In order to determine the origin of the structures, lithologies and fabrics of the Hvideklint section, the laboratory and field data previously described are analysed in detail below.

4.1 Origin of the Stratified Sequence

The lack of fabric data from an undisturbed portion of the section does not permit interpretation of the origin of the diamictons. Therefore granulometric, sedimentary-structural and stratigraphic data are used to interpret this section.

Granulometric data indicate that the Hvideklint sediment is a poorly-sorted, bimodally-distributed diamicton. If only these data are considered, then the range of probable origins is restricted to:

- 1) till;
- 2) debris flow (subaerial, subaqueous); and,
- 3) glaciotectonic melange.

When the sedimentary data are considered, the origin can be further narrowed down. Of these above possibilities, till can be eliminated because the sediment examined in this study exhibits well-defined bedding. The interbedded waterwashed gravels and sands are evidence for a subaqueous origin which eliminates the possibility of a subaerial debris flow i.e. "landslide". Similarly,

glaciotectonic melange can be eliminated as an origin because the laminations are continuous throughout the sequence whereas the shear laminae of a melange are discontinuous (Aber, 1980). Again, the interbedded gravels are evidence for a subaqueous origin which is not compatible with a glaciotectonic melange.

By elimination a subaqueous debris flow origin is postulated for this diamicton. This hypothesis is supported by the stratigraphic association with the sands and silts which conformably overlies the diamictons. Debris flow deposits have been described from many areas where they are interbedded with outwash, kame or glaciolacustrine deposits (Hartshorn, 1963; Hester and DuMontelle, 1971; Hicock et al., 1981; de Jong and Rappol, 1983). The combination of granulometric, sedimentary and stratigraphic data offers clear evidence that these deposits are subaqueous debris flows and that they have not been directly affected by the glacier from which their sediments were most likely derived.

A glaciogenic debris flow is deposited subaqueously from the melting of debris-laden ice at the terminus of a glacier or ice sheet (Evenson et al., 1977). If the glacier is advancing then the debris flows will be overlain by basal till (May, 1977). Conversely, if the glacier is retreating then the debris flows will be overlain by outwash sands and gravels (deJong and Rappol, 1983). In

all cases, the glaciogenic debris flow facies is strictly ice-marginal.

The implications for this section, in terms of what has previously been proposed, are noteworthy. It has been previously suggested for the Hvideklint section that the chalk allochthon was emplaced and that the ice sheet then continued to advance over it without pausing (Berthelsen, 1979b, Aber, 1980). Furthermore, it has also been suggested that the chalk allochthons were emplaced through a process of proglacial thrusting (Berthelsen, 1979b; Aber, 1982). Both the presence of chalk in the sediment and the location immediately adjacent to the chalk allochthon suggest that the debris flows were derived from the same ice sheet which transported the chalk allochthon. Because the debris flows occur on the lee side of the allochthon and because such debris flows are ice-marginal, the ice sheet must have completely covered the chalk. There is no evidence that any of the sediments or debris have been "bulldozed" in front of the allochthon. This signifies that the chalk allochthon must have been transported en- or sub-glacially, as some authors suggest (Banham, 1975; Moran, 1971) and not pushed in front of the advancing ice as others suggest (Aber, 1982; Rotnicki, 1976).

The stratigraphic association of sands and silts above the diamicton can be taken as evidence that the ice sheet was receding (de Jong and Rappol, 1983). Therefore, it is reasonable to infer that emplacement of the chalk

allochthon was initiated when the ice began its retreat. It is improbable that an advancing ice sheet would deposit the chalk allochthon and then continue to advance over it because some factor must initiate the emplacement of the allochthon.

4.2 State of Strain

Little work has been done on the variations in fabric through folds which are the product of glaciotectonic deformation. One study (Nielsen, 1982) examines the variation in pebble fabrics through a large recumbent fold in western Sjælland, Denmark. Through the use of a synoptic fabric diagram which plots all of the fabric results on a single stereonet without correcting for bedding orientation, Nielsen (1982) demonstrated that the original fabric has been reoriented through deformation by rotation about the fold axis only. Thus the fabric data are distributed in a girdle. Synoptic diagrams for the sediment investigated in this study reveal a different pattern (Figure 4.1). The well-defined maxima and minima directions suggest that the AMS fabric has been reoriented by some other mechanism.

The AMS of rocks is becoming increasingly popular as a petrofabric indicator for the determination of strain in deformed rocks. It is known that the AMS tensor is very sensitive to small deformations (e.g., Gravenor et al., 1984), and thus can be used as an indicator of the relative strains recorded in a single rock unit (Kligfield et al., 1977; Hrouda, 1979). The AMS does not, however, estimate the strain quantitatively because most rocks have a prestrained non-random fabric and because the AMS tensor itself is very complex which does not lend itself to simple mathematical treatment. Strains have been calculated from

AMS data (Rathore and Henry, 1982; Rathore, 1979) but this requires knowledge of the pre-strain state of the rock and the actual strain at some locality to which the AMS may be correlated. The Hvideklint site does not allow such quantitative strain analysis because neither of these two conditions can be satisfied.

The three principal susceptibility axes can be used to estimate the orientation of the strain ellipsoid during deformation. In the upper fold at Hvideklint, the X-Y plane of the strain ellipsoid is oriented with the axis of maximum elongation parallel to the fold axis and the intermediate axis dipping steeply to the north (Blocks 02-04). The fact that the intermediate axis is not significantly reoriented around the fold axis, is indicative of penetrative deformation of the type which causes the development of slaty cleavage in slates (Hrouda, 1976, 1978).

The fabric parameters, especially the ellipticity, can be used to approximate the changes in shape of the strain ellipsoid through the folds. The ellipsoid is prolate in the upper fold (Blocks 02 and 03) but becomes oblate in the lower fold (Blocks 05 and 06). This pattern is strikingly similar to the type of change which occurs when homogeneous shortening is superimposed onto a preexisting fold (Hobbs et al., 1976; see their Figure 4.33, p. 194). How the upper fold could have escaped the additional shortening which the lower fold experienced is difficult to explain.

It is reasonable to assume, however, that this secondary shortening must have occurred contemporaneously with the development of the upper fold. Comparison with the fabric distributions within the flow fold from the Scarborough section provides insight into this discrepancy. The magnetic lineations and foliations from the Scarborough flow fold when plotted on an axis-normal section (Figure 3.15) show that the stronger lineations occur near the top of the fold in the upper portion of the hinge, while the stronger foliations occur immediately below these high lineations in the centre of the hinge area itself.

The distribution described above for the Scarborough section occurs presumably as a result of the mechanism which creates the flow fold. The strong lineations at the top result from a compressional flow regime which occurs in the upper portion of the flowing layer (Enos, 1977). As the compression results in a thickening of the layer at the site of the developing fold hinge, the mass of this debris compresses the material immediately subjacent to it. As flow continues, the fold area will roll along much like a conveyor belt with the upper material being forced down into the hinge area and the material which previously occupied this position moving down into the base. It can be seen from the photograph of the Scarborough debris flow (Plate 3.5) that a sand lamination is continuous around the fold and that it exhibits microfolding in the hinge area.

The distribution of AMS ellipsoid shapes in the Hvideklint section shows a remarkably similar pattern (Figure 4.2). In both the Hvideklint sequence and the Scarborough flow fold, the variation of ellipsoid shapes in the hinge region of the fold is initially oblate, becomes constricted to prolate high in the upper hinge area, then becomes oblate again in the hinge area proper, and finally at the final stage the ellipsoid becomes greatly flattened underneath the fold. This distribution of fabrics is quite different from that observed in consolidated rocks folded by geotectonic processes (Ball, 1960).

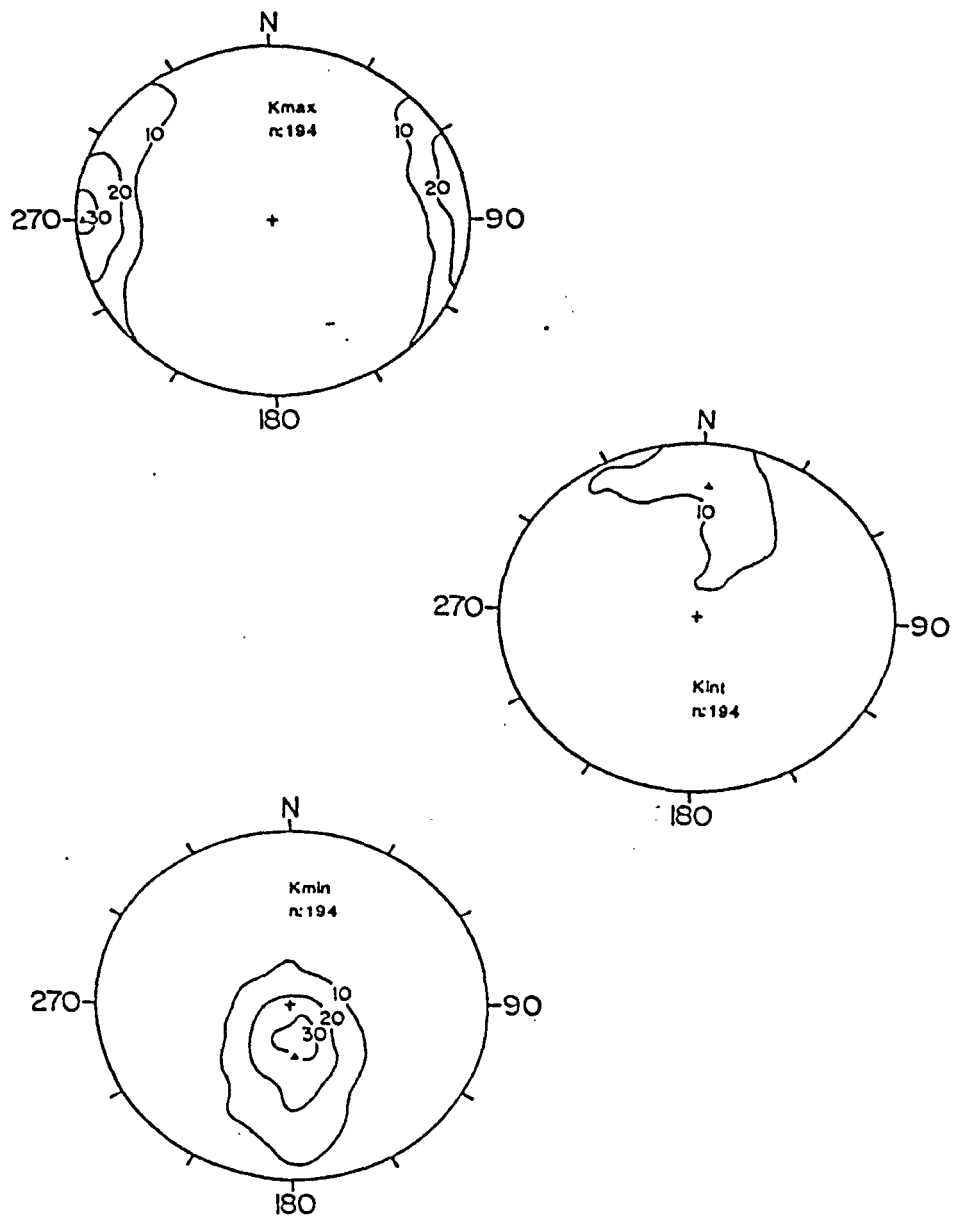


Figure 4.1 Synoptic Fabric Diagram, Hvideklint.

The data are from the folds only, Block 09 is excluded. Area of smoothing circle is 2%. The contour interval is in percent. The solid triangles are the mean directions.

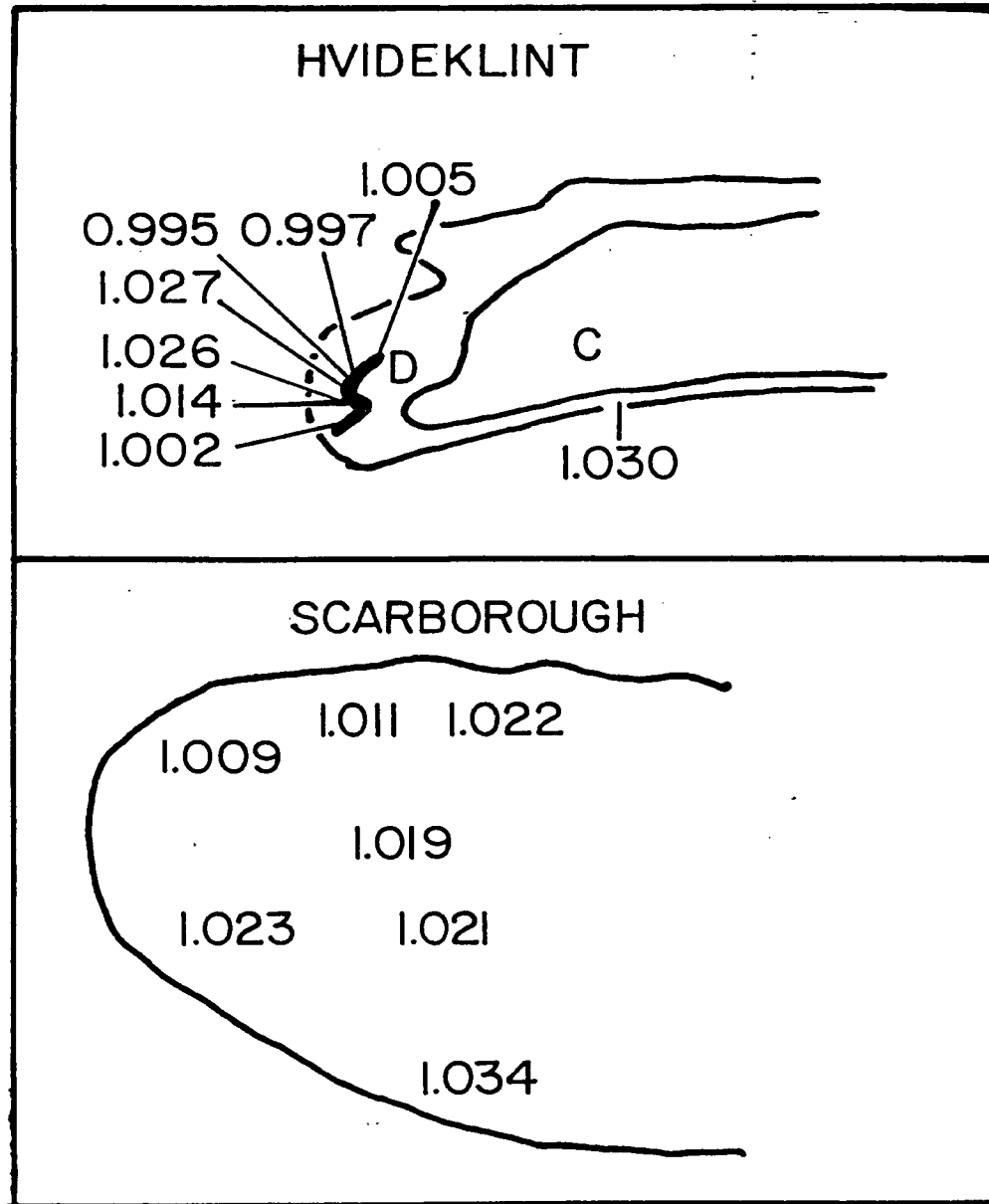


Figure 4.2 The Distribution of the Block Mean Values of Ellipticity in both the Hvideklint and Scarborough Folds.
The Hvideklint section has been simplified for clarity. The two sections are at different scales.
C is chalk, D is diamicton.

4.3 Mechanism of Folding at Hvideklint

The folded sequence at Hvideklint remains attached to the main chalk allochthon. The surface upon which the folded sequence rests is very shallowly dipping towards this chalk cliff. Clearly, these deformations cannot have occurred as a result of unconfined flow down a paleoslope as a debris flow does. A mechanism must therefore be found which can account for the similarities between the folding observed in the Hvideklint and Scarborough areas.

The study of glaciotectonics has, in general, concentrated on thrust faulting. Folding is often considered to be a secondary process and is often related to the emplacement of the thrust slices. Two processes have been proposed for the development of glaciotectonic folding that are not directly related to thrusting: i) subglacial shearing (Aber, 1982); and ii) mobilisation of subglacial sediments in response to differential loading (Berthelsen, 1979; Rotnicki, 1976). The first theory is of limited value because the shear strength of ice is too small to account for deformations on this scale (Hobbs, 1974). Second, subglacial shear is generally confined to a relatively thin layer in the uppermost basal materials, when present (Boulton and Jones, 1979). Furthermore, folds which do result from subglacial shear verge in an up-glacier direction (Nielsen, 1981). The folds at Hvideklint are verging in the opposite direction.

Examination of the chalk which comprises the core of the deformed sequence reveals that it has been intensely brecciated. Plate 4.1 shows the chalk core where it can be seen that the flint nodules (black spots) are randomly oriented. In the main chalk allochthon, these nodules are confined to well-defined bedding planes. Closer inspection (Plate 4.2) reveals that the chalk has been ground to a fine paste which was so weak that a clayey diamicton was injected under the pressure of deformation.

Van der Wateren (1981) uses the deformation behaviour of lime mud (drewite) as an indicator of the behaviour of chalk when stressed, because there is no known geotechnical work that has been done on the chalk of Møn. The independent work on lime mud (Terzaghi, 1940) shows that fine grained carbonate rocks such as chalk or drewite possess unique properties when stressed. First, a lime mud is very weak with a strength roughly equal to that of an unconsolidated Pleistocene lacustrine clay. Second and more importantly, lime mud becomes progressively weaker beyond a given pressure which is unlike ordinary clays or sands. Terzaghi (1940) attributes this contrary behaviour to the initiation of cataclasis -- the breaking of the sediment's clasts. Such cataclasis has evidently occurred in the deformed chalk of the Hvideklint sequence. Krogh (1923) has observed that unconsolidated unfrozen clays begin to flow ductilely under sufficiently high pressures. The properties of the chalk with respect to the flow limit

are unknown. However, if the values given by Krogh (1923) of 80 to 100 atmospheres are considered, then the ductile flow of an unfrozen clay layer can be initiated under an ice thickness of less than 1000 metres. The fact that lime mud behaves similarly to clay at low confining pressures, coupled with the observed decrease in the strength as the pressure increases, permits the conclusion that an unfrozen chalk could deform by ductile flow under a glacier. The thickness of the ice could be much less than 1000 metres, confining the deformation to an area near the terminus of the advancing ice where the slope of the ice sheet's surface is greatest.

This theory implies that the deformation is initiated in the layer of weaker chalk. The surrounding strata are carried along passively as the incompetent layer is extruded forward towards a zone of lower confining pressure i.e. towards the terminus of the glacier.

Even at the terminus of an ice sheet, the slope of the ice surface would be much too low to be the sole cause of the deformations. The orientation of the fold axes perpendicular to the presumed location of the ice margin suggests that the ice sheet does exert some control over the directional development of these deformations.

Consideration cannot focus solely on the slope of the immediately superjacent ice. When the entire ice sheet is considered, thicker ice which may be several kilometres back of the margin will exert a force in the marginal area

in the form of lateral stresses (Figure 4.3; Rotnicki, 1976). A region of glaciotectionic folding is created beneath the terminus of the glacier. A zone of ductility in the underlying sediments exists because the confining pressure of the overlying ice does not permit brittle deformation (Berthelsen, 1979b; Rotnicki, 1976). This model applies to the deformations of the Hvideklint because the large-scale ice slope is responsible for the directional control which is evident in the folding. The plane upon which the fold then advanced would correspond to one of the isolines of vertical compression (Rotnicki, 1976) which exist beneath the terminus of the ice.

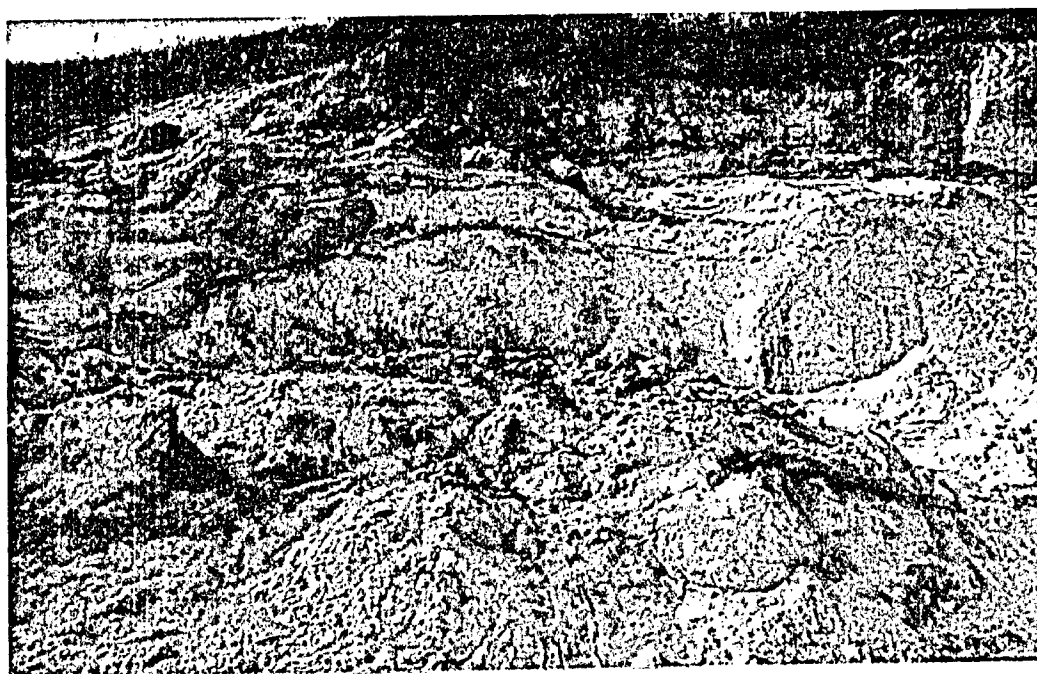


Plate 4.1 The chalk (centre) showing the lack of preferred orientation of the flint nodules (dark spots).

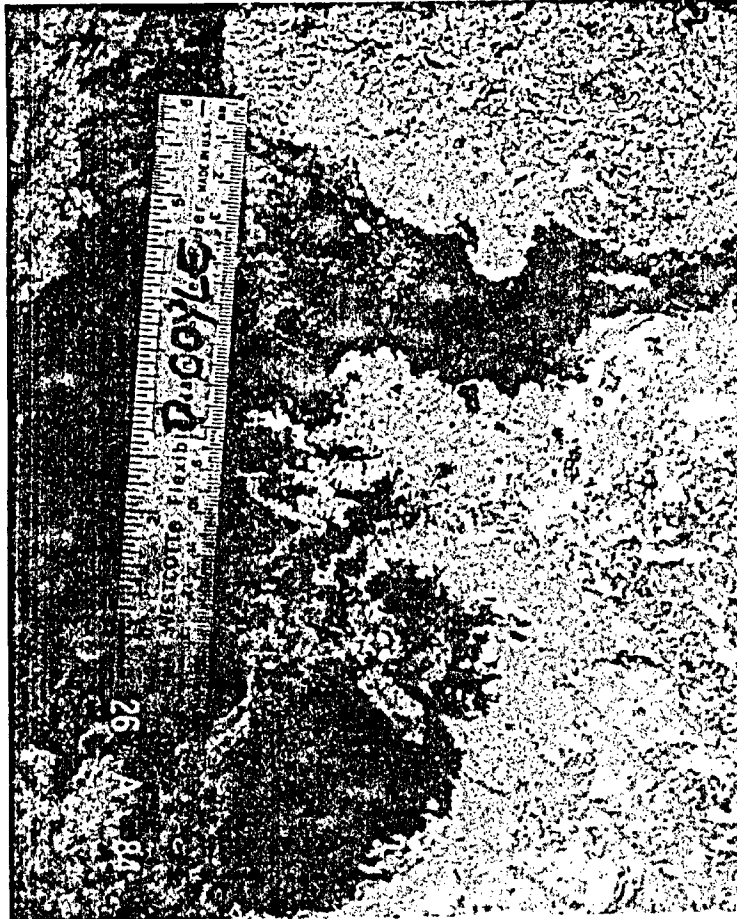


Plate 4.2 Detail of the chalk - diamicton contact. The section is vertical, and southwest is to the left.

4.4 Associated Deformations

On the island of Møn it has been assumed that deformation occurred in permafrozen sediments (e.g. Aber, 1980, 1982). Careful examination of the Hvideklint and some of the other exposures on Møn reveals several more examples of the same type of pressure-induced folding as described above.

Southwest from Hvideklint where the chalk is no longer present in the cliff, the structures shown in Plates 4.3 and 4.4 were encountered. Plate 4.3 shows a "wave" of diamicton developed in outwash sand. Plate 4.4 shows the structures immediately suprajacent to those in Plate 4.3, where the sands which were deformed by the lower diamicton have themselves been intruded into a suprajacent diamicton. Both of these structures are overturned to the southwest in the direction of ice movement. Plates 4.5 and 4.6 show two more examples of pressure-induced flow folding. Both of these sections are from the northeast coast of Møn, to the west of the very large scale deformations of Møns Klint. In both of these folds the cores are clay-rich diamicton.

Several other features from the Hvideklint section itself are worth noting. One of these has already been illustrated in Plate 4.2. The dendritic nature of this injection "flame" and its irregular edges are evidence of a viscous state for both of the materials involved. Plate 4.7 shows a diamictic dike which has been intruded into the

chalk allochthon. The dike ends approximately 15 m up into the chalk before reaching the upper contact of the chalk allochthon. Such a feature is an indication that the ice which emplaced the chalk was transgressing over unfrozen ground. Plate 4.8 shows the contact between the chalk and an overlying diamicton near the central portion of Hvideklint. The contact between chalk and diamicton is gradational, which exhibits no evidence of shearing or preferred orientations. The gradational zone has a thickness of approximately 1 m. The high chalk and low magnetic mineral content prevented the use of AMS to investigate the origin of this gradational contact so that its precise origin is uncertain. Most probably it was developed in unfrozen materials under the influence of an elevated pore water pressure at some distance behind the ice margin.

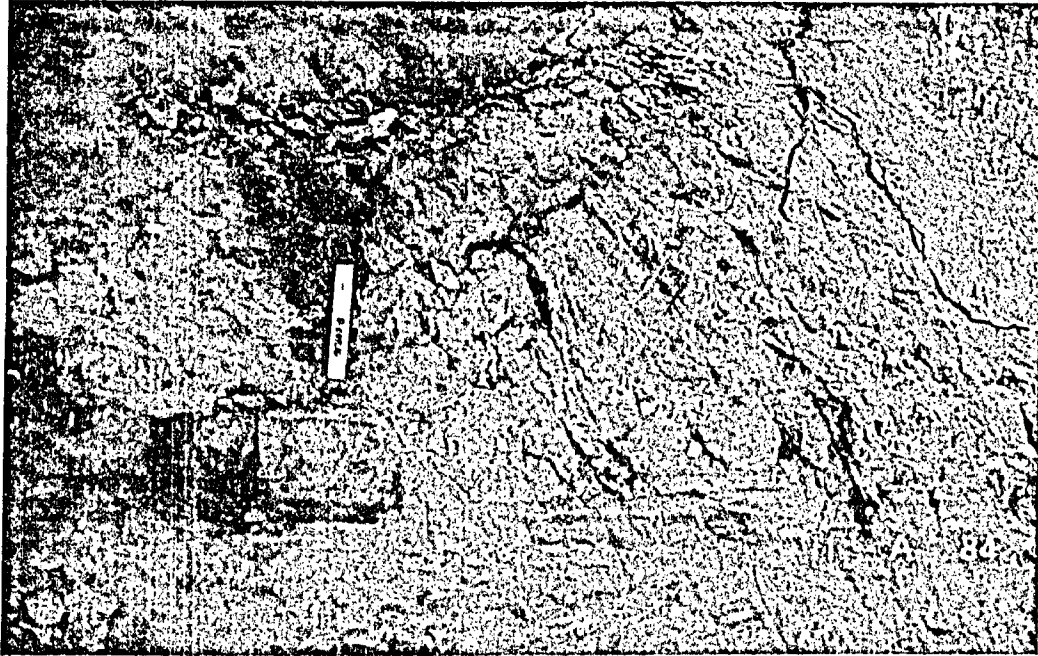


Plate 4.3 Deformations in an Outwash-Diamicton Sequence Southwest of Hvideklint. A wave-shaped body of blue-grey diamicton can be seen, which is enclosed in reddish-grey sands. The "wave" is overturned towards the southwest (left of photograph). Note the horizontal base of the wave, and how it is continuous across the area of the photograph. The ruler is 15 cm long.



Plate 4.4 Deformations above those pictured in Plate 4.3. Two "fingers" of sand (buff-brown) are intruded upwards and into diamicton (blue-grey, with oxide stain and chalk pebbles). The scale is the same as that in Plate 4.3. Note that in this photograph and Plate 4.3 the presumed ice-movement direction was from right to left.



Plate 4.5 Folding in a Diamicton Sequence Northwest of Møns Klint. Pictured is a large (3 metre high) upright asymmetric fold, the left limb of which is pinched into an acute angle at the lower right.



Plate 4.6 Folding in a Diamicton Sequence Northwest of Møns Klint. Pictured is a small (0.8 metre recumbent asymmetric fold. The lower limb of this fold is sharply pinched into an acute angle of less than 20° . Note that the lamination is not destroyed, and that the fold is not sheared off or faulted in the area of the pinched fold on the lower limb.

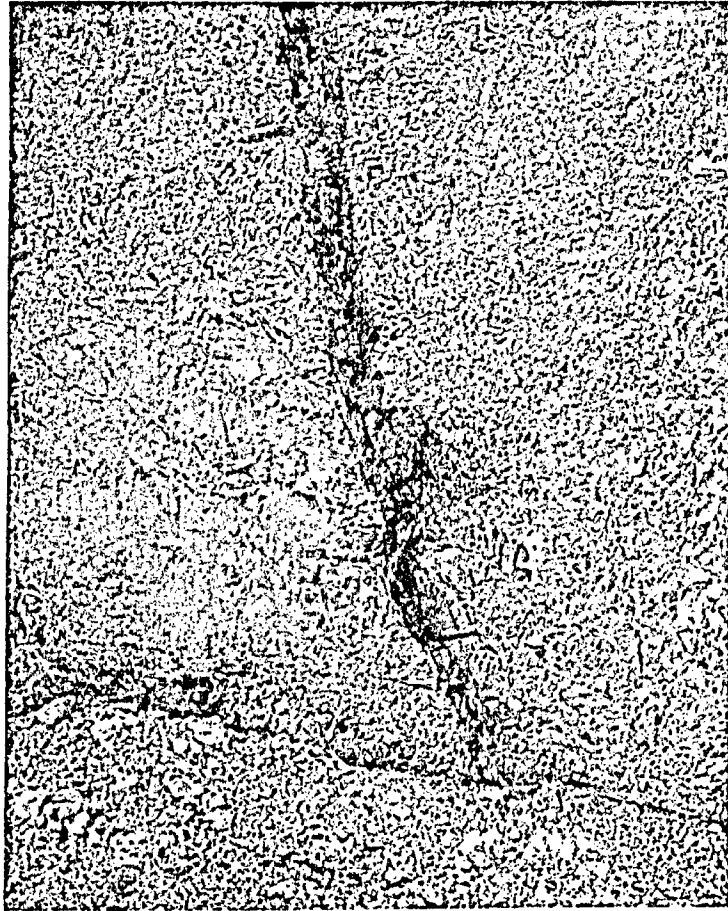


Plate 4.7 Diamicton Dike, Hvideklint. The dike of sandy diamicton (dark) has apparently been intruded upwards into the chalk cliff (white). The pencil is approximately 18 cm long.

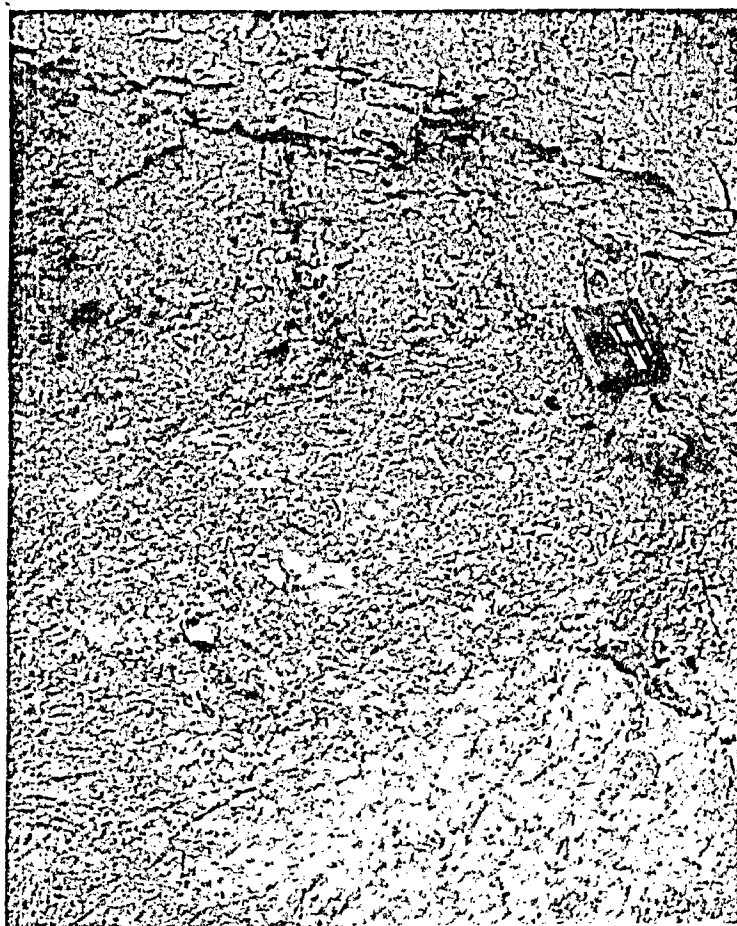


Plate 4.8 Gradational Contact between Chalk and Diamicton, Hvideklint. Pictured is a gradational zone between the overlying diamicton (blue-grey) and the chalk cliff (bottom, white). Note the absence of preferred orientations or evidence of shear in the gradational zone.
The book is 20 cm long.

4.5 Frozen or Unfrozen?

Previous workers on the Hvideklint section have interpreted the deformations to have taken place in permafrozen sediments (Aber, 1980; Berthelsen, 1979b). Evidence presented in this study suggests that some of the deformations must have occurred in sediments which were not permafrozen. It must be stressed at this point that the following interpretations refer only to the deformed sediments which were sampled and examined in detail in this study. No attempt should be made to try to relate these interpretations to other glaciotectonic phenomena found at or near the Hvideklint section, especially the initial thrusting and emplacement of the largely intact chalk allochthons.

Before the sediments can be interpreted to have been frozen or unfrozen, careful consideration of these sediments and their depositional environment must be made. Previous work on the Hvideklint has assumed that the sediments in the study area were of pre-tectonic origin, being deformed during or shortly after the emplacement of the chalk allochthons (Aber, 1980). If this were true, then the assumption that these sediments were permafrozen -- as were the chalk allochthons -- may be valid. Careful examination of these sediments reveals that they were deposited only after the chalk allochthons were emplaced, because of the high content of materials which were derived from these allochthons. Deposition was by normal

fluvial/lacustrine processes and not by the development of a glaciotectonic melange. Shallow permafrost is not stable under rivers or lakes (Muller, 1947; Mackay and Mathews, 1964). Thus it can be concluded that there would not have been permafrost development during the deposition of the debris-flow and subsequent sand-silt sequences. Unfortunately the contact between the sands and the overlying Upper Dislocated Till is unconformable so that it cannot be determined whether or not there was an appreciable interval of non-deposition and possible permafrost development before the ice advanced over the area. Nevertheless it is unreasonable to make the extra assumption that the sediments were frozen on the basis of the sedimentary data.

The strength of the materials involved also raises questions about the previous assumptions of a frozen state. The relative strengths of sand, diamicton and chalk are the same regardless of whether they are frozen or unfrozen (Banham, 1975). In confined tests, sand is always markedly stronger than clay or chalk. Also unconsolidated sediments, particularly sands, remain intact during deformation and faulting even when unfrozen (van der Wateren, 1981). It was the observation that unconsolidated sediments remained intact that helped initiate the permafrost theory of glaciotectonic deformation (e.g., Mathews and Mackay, 1960; Kupsch, 1962), but recent work

has shown that a permafrozen state is not necessary to accomplish this (van der Wateren, 1981).

The Hvideklint sediments do not show evidence of brittle behaviour? The chalk in particular exhibits extreme ductile deformation. This study also presents data from a fold in a debris flow. From examination of Plate 3.5, it can be clearly seen that a sand layer retains its original bedding even when the deformation was unconfined flow. The confining pressure of the overlying sediments and ice at Hvideklint would have been more than sufficient to maintain the stratal continuity which is observed in the higher parts of the section. The assumption that a permafrozen state is required to maintain stratal continuity is obviously invalid.

It is clear now that the sediments do not need to have been frozen during deformation. Arguments concerning the origin of the sediments indicated that there is a strong possibility that the sediments were not permafrozen prior to deformation. Evidence should now be sought which will establish conclusively whether the sediments were in fact frozen or unfrozen. The injection feature (Plate 4.2) and the diamicton dike (Plate 4.7) provide such evidence. There is no apparent way in which these features could have developed in permafrozen materials. Furthermore the gradational contact (Plate 4.8) is evidence that the chalk allochthon itself was unfrozen at some point, at least at its edges. Whether the chalk allochthon was frozen or not

at the time of thrusting is beyond the consideration of this study.

4.6 Model for the Origin of the Sequence at Hvideklint

A model for the origin of this section is presented in Figure 4.4. There are four main stages to this model.

1) The main chalk allochthon is emplaced. The ice completely covered the chalk, and a debris- and chalk-rich zone is present immediately adjacent to the allochthon.

2) Melting of the ice results in the deposition of the subaqueous debris flow - outwash sequence. The debris flows represent the early melting of the debris-laden ice margin. As the margin recedes, the sediments deposited from meltwaters become better sorted as a result of the increase in travel distance so that sands and silts are deposited above the debris flows.

3) The Northeast Ice readvances over the area. While still in the steeply-sloping marginal zone of the glacier, the pressure of the overriding ice initiates ductile flow in the weak chalk. The relative weakness of the immediately adjacent chalk-rich debris flows provides a convenient site into which the chalk may flow. Directional control is provided by the decreasing confining pressure towards the ice margin and by a high lateral pressure exerted by the greater ice thicknesses upstream.

4) Equilibrium is reached when the ice continues to advance over the sequence. The lateral pressure gradient will decrease as the thickness of ice increases. Strain hardening in the sands (Hubbert, 1951) may contribute to the equilibrium by making the sequence more resistant to

stress but this cannot be proven. At this point the folded sequence has assumed its present morphology. Deposition of the Upper Dislocated Till begins.

Several additional comments are in order. First, in the initial stage of deformation, (see #3 in Figure 4.4) the sequence resembles the two folds from Møns Klint shown in Plates 4.5 and 4.6. The existence of these two other folds confirms that this mechanism of glaciotectonic folding is not unique to the Hvideklint section. Second, the fact that deformation of the chalk is confined only to the margin of the allochthon allows the possibility that the core of the allochthon has remained frozen since its initial emplacement. Conversely, the deformation may be localised at the margin because of the transmittance of stress through the allochthon. This situation is analogous to the transmittance of stress through a row of billiard balls. Only the ball at the far end exhibits movement in response to the stress applied at the opposite end of the row.

In summary this model is meant to be only an approximate guide to the development of the deformation which exists in the Hvideklint section. A more detailed analysis including fabric studies of all deformed strata and a more detailed investigation of the engineering properties of these materials are required before a complete picture of the events and processes preserved in the sequence can be drawn. One of the future studies with

great potential would be the examination of the stress behaviour of the chalk because a detailed knowledge of this could lead to determination of the thickness of the ice sheet which initiated the deformation.

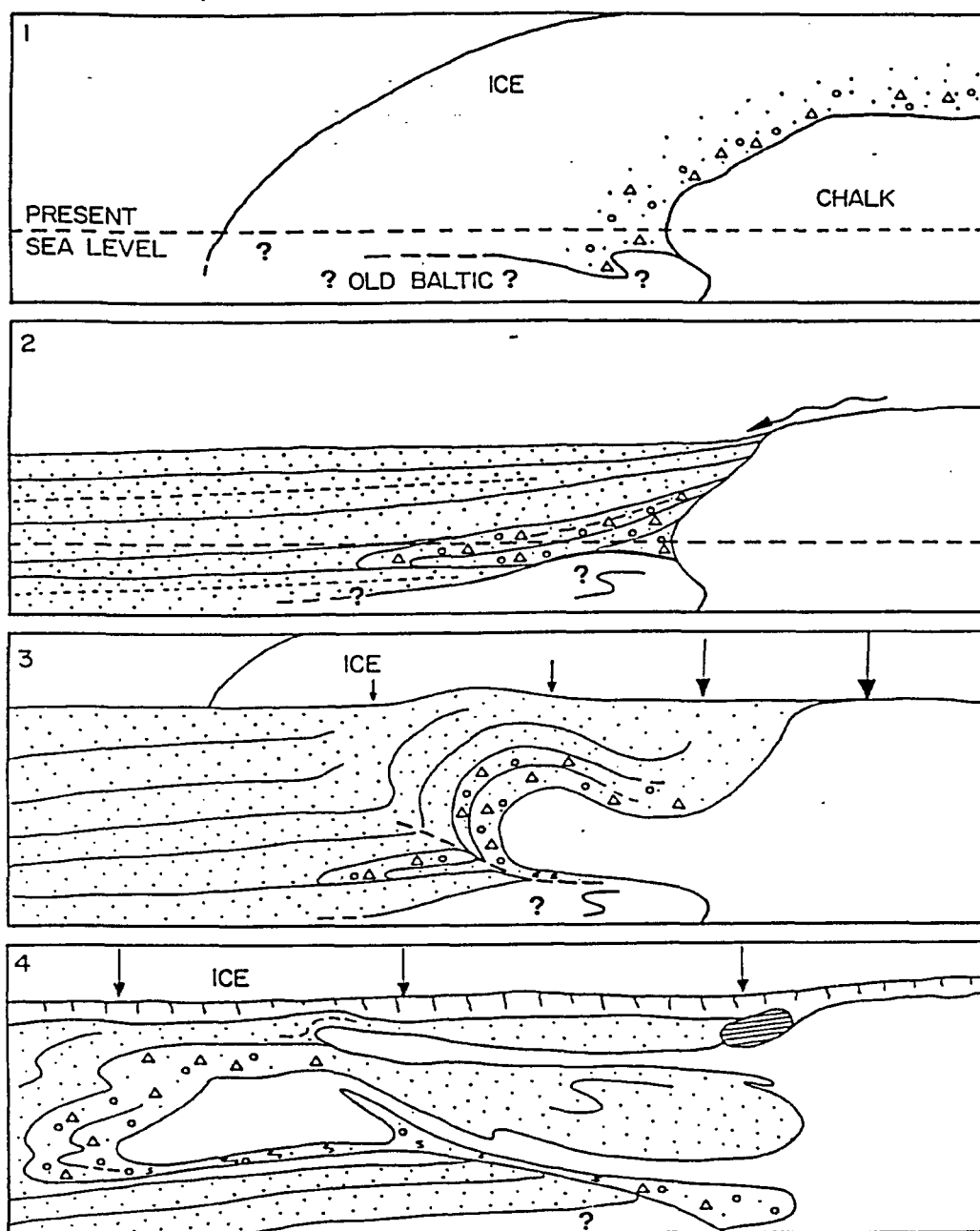


Figure 4.4 Model of the Origin of the Folding at Hvideklint.

The position of the ice is for illustrative purposes only. The precise location is not to be inferred. Lithologies are the same as in Figure 3.1. See text for details.

- Dreimanis, A. 1984. Comments and Reply on "Sedimentation in a large lake: a reinterpretation of the late Pleistocene stratigraphy at Scarborough Bluffs, Ontario, Canada. *Geology*, v. 92, pp. 185-186.
- Enos, P. 1977. Flow regimes in debris flow. *Sedimentology*, v. 24, pp. 133-142.
- Evenson, E.B., Dreimanis, A., and Newsome, J.W. 1977. Subaquatic flow tills: a new interpretation for the genesis of some laminated till deposits. *Boreas*, v. 6, pp. 115-133.
- Eyles, C., and Eyles, N. 1983. Sedimentation in a large lake: a reinterpretation of the late Pleistocene stratigraphy at Scarborough Bluffs, Ontario, Canada. *Geology*, v. 11, pp. 146-152.
- Fisher, R.A. 1953. Dispersion on a sphere. *Royal Society of London, Proceedings., Ser. A*, v. 217, pp. 295-305.
- Gravenor, C.P. 1985a. Magnetic and pebble fabrics of glaciomarine diamicton in the Champlain Sea, Ontario, Canada. *Canadian Journal of Earth Sciences*, v. 22, no. 3, pp. 422-434.
- Gravenor, C.P. 1985b. Glacial tectonic and flow structures in glaciogenic deposits: a cautionary note. *Bulletin of the Geological Society of Denmark*, v. 34, pp. 3-11.
- Gravenor, C.P., Symons, D.T.A, and Coyle, D.A. Errors in the anisotropy of magnetic susceptibility and magnetic remanence of unconsolidated sediments, produced by sampling methods. *Geophysical Research Letters*, v. 1, no. 9, pp. 836-839.
- Hamilton, N., and Rees, A.I. 1970. The use of magnetic fabric in paleo-current estimation. In *Paleogeophysics. Edited by S.K. Runcorn. Academic Press, New York, NY*, pp. 445-464.
- Hansen, S. 1965. The Quaternary of Denmark. In *The Quaternary, Vol. 1. Edited by K. Rankama. Interscience, New York*. pp. 1-90.
- Hartshorn, J.H. 1963. Flowtill in southeastern Massachusetts. *Geological Association of America Bulletin*, v. 69, pp. 477-482.

- Hester, N.C., and DuMontelle, P.B. 1971, Pleistocene mudflow along the Shelbyville moraine front, Macon County, Illinois. In Till, a Symposium. Edited by R.P. Goldthwaite. Ohio State University Press, pp. 367-382.
- Hicock, S.R., Dreimanis, A., and Broster, B.E. 1981. Submarine flow tills at Victoria, British Columbia. Canadian Journal of Earth Sciences, v. 18, pp. 71-80.
- Hobbs, B.E., Means, W.D., and Williams, P.F. 1976. An Outline of Structural Geology. John Wiley and Sons, New York. 571 pp.
- Hobbs, P.V. 1974. Ice Physics. Clarendon Press, Oxford, 820 pp.
- Houmark-Nielsen, M, and Berthelsen, A. 1981. Kineto-stratigraphic evaluation and presentation of glacial-stratigraphic data, with examples from northern Samsø, Denmark. Boreas, v. 10, pp. 411-422.
- Hrouda, F. 1976. A model for the orientation process of ferromagnetic minerals in slates. Earth and Planetary Science Letters, v. 33, pp. 107-110.
- Hrouda, F. 1978. The magnetic fabric in some folds. Physics of the Earth and Planetary Interiors, v. 17, pp. 89-97.
- Hrouda, F. 1979. The strain interpretation of magnetic anisotropy in rocks of the Nizky Jeseník Mountains (Czechoslovakia). Sborník geologie ved - UG, v. 16, pp. 27-65.
- Hrouda, F. 1982. Magnetic anisotropy of rocks and its application in geology and geophysics. Geophysical Surveys, v. 5, pp. 37-82.
- Hrouda, F., Janak, F., Rejl, L., and Weiss, J. 1971. The use of magnetic susceptibility anisotropy for estimating the ferromagnetic mineral fabrics of metamorphic rocks. Geologisches Rundschau, v. 60, pp. 1124-1142.
- Hubbert, M.K. 1951. Mechanical basis for certain familiar geologic structures. Geological Society of America, Bulletin. v. 62, pp. 355-372.
- Jong, M.G.G. de, and Rappol, M. 1983. Ice-marginal debris-flow deposits in western Allgäu, southern West Germany. Boreas, v. 12, pp. 57-70.

- Karrow, P.F. 1967. Pleistocene Geology of the Scarborough Area. Ontario Department of Mines, Geological Report 46, 108 pp.
- Karrow, P.F. 1984a. Comments and Reply on "Sedimentation in a large lake: a reinterpretation of the late Pleistocene stratigraphy at Scarborough Bluffs, Ontario, Canada. *Geology*, v.92, p. 185.
- Karrow, P.F. 1984b. Lithofacies types and vertical profile models: an alternative approach to the description and environmental interpretation of glacial diamict and diamictite sequences: Discussion. *Sedimentology*, v. 31, pp. 883-884.
- Khan, M.A. 1962. Anisotropy of magnetic susceptibility of some igneous and metamorphic rocks. *Journal of Geophysical Research*, v. 67, pp. 2873-2885.
- Kligfield, R., Lowrie, W., and Dalziel, I. 1977. Magnetic susceptibility anisotropy as a strain indicator in the Sudbury Basin, Ontario. *Tectonophysics*, v. 40, pp. 287-308.
- Krogh, J. van. 1923. Undersokelser over Norske Lerer. Staatens Rastofkomite. III., Christiania
- Kupsch, W.O. 1962. Ice-thrust ridges in western Canada. *Journal of Geology*, v. 70, no. 5, pp. 582-594.
- Mackay, J.R., and Mathews, W.H. 1964. The role of permafrost in ice-thrusting. *Journal of Geology*, v. 72, no. 3, pp. 378-380.
- Mathews, W.H., and Mackay, J.R. 1960. Deformation of soils by glacier ice and the influence of pore pressures and permafrost. *Transactions of the Royal Society of Canada*, v. 54, ser. 3, sec. 4, pp. 27-36.
- May, R.W. 1977. Facies model for sedimentation in the glaciolacustrine environment. *Boreas*, v. 6, pp. 175-180.
- Moran, S.R. 1971. Glaciotectonic structures in drift. In *Till, a Symposium*. Edited by R.P. Goldthwaite. Ohio State University Press, pp. 127-148.
- Muller, S.W. 1947. Permafrost or Permanently Frozen Ground and Related Engineering Problems. J. Edwards, Inc., Ann Arbor, Michigan.
- Nielsen, P.E. 1982. Till fabric reoriented by subglacial shear. *Geologiska Föreningens I Stockholm Förhandlingar*, v. 103, pt. 3, pp. 383-387.

- Rasmussen, L.A. 1975. Kineto-stratigraphic glacial drift units on Hindsholm, Denmark. *Boreas*, v. 4, pp. 209-217.
- Rathore, J. 1979. Magnetic susceptibility anisotropy in the Cambrian slate belt and correlation with strain. *Tectonophysics*, v. 53, pp. 83-97.
- Rathore, J.S., and Henry, B. 1982. Comparison of strain and magnetic fabrics in Dalradian rocks from the southwest Highlands of Scotland. *Journal of Structural Geology*, v. 4(3), pp. 373-384.
- Rees, A.I. 1968. The production of preferred orientation in a concentrated dispersion of elongated and flattened grains. *Journal of Geology*, v. 76, pp. 457-465.
- Rotnicki, K. 1976. The theoretical basis for and a model of the origin of glaciotectionic deformations. *Quaestiones Geographicae*, v. 3, pp. 103-139.
- Sjørring, S. 1977. The glacial stratigraphy of the island of Als, southern Denmark. *Z. Geomorph. N. F., Suppl.-Bd. 27*, pp. 1-11.
- Terzaghi, R.D. 1940. Compaction of lime mud as a cause of secondary structure. *Journal of Sedimentary Petrology*, v. 10, pp. 78-90.
- Tiara, A., and Scholle, P.A. 1979. Deposition of resedimented sandstone beds in the Pico Formation, Ventura Basin, California as interpreted from magnetic fabrics. *Geological Society of America Bulletin*, v. 90, pp. 952-962.
- Wateren, F.M. van der, 1981. Glacial tectonics at the Kwintelooljen Sandpit, Rhenen, The Netherlands. *Meded. Rijks Geol. Dienst*, v. 35-7, pp. 252-268.
- Wentworth, C.K. 1922. A scale of grade and class terms for clastic sediments. *Journal of Geology*, v. 30, pp. 377-392.
- Woldstedt, P. 1954. *Das Eiszeitalter*. Stuttgart.

APPENDIX I: SELECTED BIBLIOGRAPHY

- Abrahamsen, N., and Knudsen, K.L. 1979. Indication of a geomagnetic low-inclination excursion in supposed Middle Weichselian interstadial marine clay at Rubjerg, Denmark. *Physics of the Earth and Planetary Interiors*, v. 18, pp. 238-246.
- Abrahamsen, N., and Readman, P.W. 1980. Geomagnetic variations recorded in Older ($\approx 23\ 000$ B.P.) and Younger Yoldia Clay ($\approx 14\ 000$ B.P.) at Nørre Lyngby, Denmark. *Geophys. J. R. astr. Soc.*, v. 62, pp. 329-344.
- Andrews, D.E. 1980. Glacially thrust bed rock - An indication of Late Wisconsin climate in western New York State. *Geology*, v. 8, pp. 97-101.
- Andrews, J.T. 1971. Methods in the analysis of till fabrics. In *Till, a Symposium*. Edited by R.P. Goldthwaite. Ohio State University Press, pp. 321-327.
- Babcock, E.A., Fenton, M.M., and, Andriashek, L.D. 1978. Shear phenomena in ice-thrust gravels, central Alberta. *Canadian Journal of Earth Sciences*, v. 15, pp. 277-283.
- Boulton, G.S. 1968. Flow tills and related deposits on some Vestspitsbergen glaciers. *Journal of Glaciology*, v. 7, no. 51, pp. 391-412.
- Boulton, G.S. 1971. Till genesis and fabric in Svalbard, Spitsbergen. In *Till, a Symposium*. Edited by Goldthwaite, R.P. Ohio State University Press, pp. 41-72.
- Boulton, G.S. 1975. Processes and patterns of subglacial sedimentation: a theoretical approach. In *Ice Ages, Ancient and Modern*. Edited by A.E. and F. Moseley. Seel House Press, Liverpool, pp. 7-42.
- Boulton, G.S., Dent, D.L., and Morris, E.M. 1974. Subglacial shearing and crushing, and the role of water pressures in tills from south-east Iceland. *Geografiska Annaler*, v. 56, ser. A, no. 3-4, pp. 135-145.
- Brinkmann, R. 1953. Über die diluvialen Störungen auf Rügen. *Geologische Rundschau*, B. 41, Sonderband, pp. 231-241.

- Byers, A.R. 1959. Deformation of the Whitemud and Eastend formations near Claybank, Saskatchewan. Transactions of the Royal Society of Canada, v. 53, ser. 3, sec. 4, pp. 1-11.
- Dvorak, J., and Hroudá, F. 1972. The origin of tectonic structures in weakly metamorphosed sediments, as studied by magnetic susceptibility. Neues Jahrbuch für Geologie und Paläontologie Monatshefte, H. 12, pp. 703-712.
- Evenson, E.B. 1971. The relationship of macro- and microfabric of till and the genesis of glacial landforms in Jefferson County, Wisconsin. In Till, a Symposium. Edited by R.P. Goldthwaite. Ohio State University Press, pp. 345-364.
- Glen, J.W., Donner, J.J., and West, R.G. 1957. On the mechanism by which stones in till become oriented. American Journal of Science, v. 255, pp. 194-205.
- Gravenor, C.P., and Stupavsky, M. 1975. Convention for reporting magnetic anisotropy of till. Canadian Journal of Earth Sciences, v. 12, no. 6, pp. 1063-1069.
- Holm, P.E. 1983. The effect of strain heterogeneity on graphical strain analysis methods. Tectonophysics, v. 95, pp. 101-110.
- Hroudá, F., and Janák, F. 1976. The changes in shape of the magnetic susceptibility ellipsoid during progressive metamorphism and deformation. Tectonophysics, v. 34, pp. 135-148.
- Hroudá, F., Janák, F., and Rejl, L. 1978. Magnetic anisotropy and ductile deformation of rocks in zones of progressive regional metamorphism. Gerlands Beitr. Geophysik, Leipzig, v. 87, no. 2, pp. 126-134.
- Hubbert, M.K. 1951. Mechanical basis for certain familiar geologic structures. Geological Society of America Bulletin, v. 62, pp. 355-372.
- Jeffery, G.B. 1922. The motion of ellipsoidal particles immersed in a viscous fluid. Royal Society of London, Proceedings, Ser. A, v. 102, pp. 161-179.
- Kodama, K.P., and Cox, A. 1978. The effects of a constant volume deformation on the magnetisation of an artificial sediment. Earth and Planetary Science Letters, v. 38, pp. 436-442.

- Köster, R. 1957. Schuppung und Faltung im glazialtektonischen Experiment. *Geologisches Rundschau*, v. 46, pp. 564-571.
- Krüger, J., and Marcussen, I. 1976. Lodgement till and flow till: a discussion. *Boreas*, v. 5, pp. 61-64.
- Kulhawy, F.H. 1975. Stress deformation properties of rock and rock discontinuities. *Engineering Geology*, v. 9, pp. 327-350.
- Lawson, D.E. 1979. A comparison of the pebble orientations in ice and deposits of the Matanuska Glacier, Alaska. *Journal of Geology*, v. 87, pp. 629-645.
- Mandl, G., Jong, L.N.J. de, and Maltha, A. 1977. Shear zones in granular material. *Rock Mechanics*, v. 9, pp. 95-144.
- March, A. 1932. Mathematische Theorie der Regelung nach der Korngestalt bei affiner Deformation. *Z. Kristallogr.*, v. 81, pp. 285-297.
- Marcussen, I. 1973. Studies on flow till in Denmark. *Boreas*, v. 2, pp. 213-231.
- Marcussen, I. 1975. Distinguishing between lodgement till and flow till in Weichselian deposits. *Boreas*, v. 4, pp. 113-123.
- Mark, D.M. 1973. Analysis of axial orientation data, including till fabrics. *Geological Society of America Bulletin*, v. 84, pp. 1369-1374.
- Mark, D.M. 1974. On the interpretation of till fabrics. *Geology*, v. 2, pp. 101-104.
- Mathews, W.H. 1964. Water pressure under a glacier. *Journal of Glaciology*, v. 5, no. 38, pp. 235-240.
- Mathews, W.H. 1974. Surface profiles of the Laurentide ice sheet in its marginal areas. *Journal of Glaciology*, v. 13, pp. 37-43.
- May, R.W., Dreimanis, A., and Stankowski, W. 1980. Quantitative evaluation of clast fabrics within the Catfish Creek Till, Bratville, Ontario. *Canadian Journal of Earth Sciences*, v. 17, pp. 1064-1074.
- Mörner, N.A., Floden, T., Beskow, B., Elhammer, A., and Haxner, H. 1975. Late Weichselian deglaciation of the Baltic. *Baltica*, v. 6, pp. 33-51.

- Nye, J.F. 1952. A method of calculating the thickness of the ice sheets. *Nature*, v. 169, pp. 529-530.
- Nye, J.F. 1957. The distribution of stress and velocity in glaciers and ice-sheets. *Royal Society of London Proceedings, Ser. A*, v. 239, pp. 113-133.
- Rees, A.I. 1979. The orientation of grains in a sheared dispersion. *Tectonophysics*, v. 55, pp. 275-287.
- Ruegg, G.H.J. 1981. Ice-pushed Lower and Middle Pleistocene deposits near Rhenen (Kwintelooijen): sedimentary-structural and lithological/granulometrical investigations. *Meded. Rijks Geol. Dienst*, v. 35-2, pp. 165-177.
- Rutten, M.G. 1960. Ice-pushed ridges, permafrost and drainage. *American Journal of Science*, v. 258, pp. 293-297.
- Sanderson, D.J., and Meneilly, A.W. 1981. Analysis of strain modified uniform distributions: andalusite fabrics from a granite aureole. *Journal of Structural Geology*, v. 3(2), pp. 109-116.
- Selsing, L. 1981. Stress analysis on conjugate normal faults in unconsolidated Weichselian glacial sediments from Brorfelde, Denmark. *Boreas*, v. 10, pp. 275-279.
- Slater, G. 1926. Glacial tectonics as reflected in disturbed drift deposits. *Proceedings of the Geological Association*, v. 37, pt. 4, pp. 392-400.
- Stupavsky, M., and Gravenor, C.P. 1974. Water release from the base of active glaciers. *Geological Society of America Bulletin*, v. 85, pp. 433-436.
- Stupavsky, M., and Gravenor, C.P. 1975. Magnetic fabric around boulders in till. *Geological Society of America Bulletin*, v. 86, pp. 1534-1536.
- Symons, D.T.A, Stupavsky, M., and Gravenor, C.P. 1980. Remanence resetting by shock-induced thixotropy in the Seminary Till, Scarborough, Ontario, Canada. *Geological Society of America Bulletin*, v. 91, pp. 593-598.
- Taylor, G.I. 1923. The motion of ellipsoidal particles in a viscous fluid. *Royal Society of London Proceedings, Ser. A*, v. 103, pp. 58-61.

- Thompson, R. 1978. European paleomagnetic secular variation 13,000 - 0 B.P. *Polskie Archiwum Hydrobiologii*, v. 25, pp. 413-418.
- Thompson, R., and Berglund, B. 1976. Late Weichselian geomagnetic "reversal" as a possible example of the reinforcement syndrome. *Nature*, v. 263, pp. 490-491.
- Verosub, K. 1975. Paleomagnetic excursions as magnetostratigraphic horizons: a cautionary note. *Science*, v. 190, pp. 48-50.
- Willis, D.G. 1977. A kinematic model of preferred orientation. *Geological Society of America Bulletin*, v. 88, pp. 883-894.
- Woodcock, N.H. 1977. Specification of fabric shapes using an eigenvalue method. *Geological Society of America Bulletin*, v. 88, pp. 1231-1236.

VITA AUCTORIS

Name: David Alexander Coyle

Date of Birth: February 12, 1963

Place of Birth: Kingston, Ontario

Parents: James H. Coyle, B.Sc., M.D., D.Psych;

Carolyn M. Coyle, R.T. (geb. Zoern)

- 1977-1978 Wexford Collegiate Institute, Scarborough,
Ontario
- 1978-1980 Scottsdale High School, Scottsdale, Arizona,
U.S.A. Graduated with Honours.
- 1980-1984 University of Windsor, Windsor, Ontario.
Graduated with an Honours B.Sc. in Geology.
- 1984-1986 University of Windsor, Windsor, Ontario.
Graduated with an M.Sc. in Geology.